PNAS
www.pnas.org

Main Manuscript for

Asteroid impact, not volcanism, caused the end-Cretaceous dinosaur extinction.

Alfio Alessandro Chiarenza[1,2*†], Alex Farnsworth[3†], Philip D. Mannion[4], Dan J. Lunt[3], Paul Valdes[3], Joanna V. Morgan[1], Peter A. Allison[1].

1 Department of Earth Science and Engineering, Imperial College London, South Kensington, London, SW7 2AZ, UK.

2 Perot Museum of Nature and Science, Dallas, Texas, 75201, USA.

3 School of Geographical Sciences, University of Bristol, Bristol, BS8 1TH, UK.

4 Department of Earth Sciences, University College London, London, Gower Street, WC1E 6BT, UK.

†These authors contributed equally to this manuscript.

*Alfio Alessandro Chiarenza.

Email: a.chiarenza15@gmail.com

ORCID ID: https://orcid.org/0000-0001-5525-6730

Classification

Classification: Biological Sciences: Evolution

Keywords

Dinosauria, Extinction, End-Cretaceous, Chicxulub, Deccan

Author Contributions

A.A.C., A.F., P.D.M., P.A.A and J.V.M. conceived and designed the research; A.A.C., A.F., D.J.L. and P. V. produced and collected data; A.A.C. and A.F. analyzed the data; A.A.C. and A.F. produced the figures; A.A.C., A. F., P.D.M., and P.A.A. wrote the manuscript. A.A.C. and A.F. contributed equally to this work. All authors provided critical comments on the manuscript

This PDF file includes:

Main Text
Figures 1 to 4
Tables 1 to 3

Abstract

The Cretaceous/Paleogene mass extinction, 66 Ma, included the demise of non-avian dinosaurs. Intense debate has focused on the relative roles of Deccan volcanism and the Chicxulub asteroid impact as kill mechanisms for this event. Here we combine fossil-occurrence data with paleoclimate and habitat-suitability models, to evaluate dinosaur habitability in the wake of various asteroid-impact and Deccan volcanism scenarios. Asteroid-impact models generate a prolonged cold winter that suppress potential global dinosaur habitats. Conversely, long-term forcing from Deccan volcanism (CO_2-induced warming) leads to increased habitat suitability. Short-term (aerosol cooling) volcanism still allows equatorial habitability. These results support the asteroid impact as the main driver of the non-avian dinosaur extinction. In contrast, induced warming from volcanism mitigated the most extreme effects of asteroid impact, potentially reducing the extinction severity.

Significance Statement

This is the first quantitative test to our knowledge of end-Cretaceous extinction scenarios and how those would have affected dinosaur habitats. Combining climate and ecological modelling tools we were able to demonstrate a substantial detrimental effect on dinosaur habitats caused by an impact winter scenario triggered by the Chicxulub asteroid. We were not able to obrain such an extinction state with several modelling outputs from Deccan volcanism. We further show that the concomitant prolonged eruption of the Deccan traps might have acted as an amelioreting agent buffering the negative effects on climate and global ecosystems that the asteroid impact produced at the Cretaceous–Paleogene boundary.

Main Text

Introduction

The end-Cretaceous mass extinction, 66 million years ago (Ma), is the most recent of Raup and Sepkoski's (1982) 'Big Five' extinction events *(1, 2)*. Non-avian dinosaurs, along with many other groups that had dominated the Earth for 150 million years, went extinct. Although there is still debate as to whether dinosaurs were already in decline *(3)* prior to their extinction, their fossil record demonstrates global survival until the terminal Cretaceous and unambiguous absence afterwards. The Cretaceous/Paleogene (K/Pg) mass extinction coincided with two major global environmental perturbations: heightened volcanism associated with the Deccan Traps, and the Chicxulub asteroid impact (Fig. 1a) *(4)*. The relative roles of these two potential kill mechanisms on the timing and magnitude of the extinction have been fiercely debated for decades *(4, 5)*. The Maastrichtian has been shown to have a relatively high climate sensitivity *(6)* meaning even relatively small perturbations to the system could potentially have a catastrophic impact.

The Deccan Traps, in present-day west-central India *(7)*, formed from a series of short (~100 kyr) intermittent eruption pulses *(8)*, with two main phases *(8, 9)* at ~67.4 Ma (towards the end of the Cretaceous) and ~66.1 Ma (starting just before the boundary and continuing through the earliest Paleogene) erupting an estimated >10^6 km^3 of magma over the duration ~710,000 years *(9, 10)*. This volcanism released radiatively active atmospheric gases, particularly carbon dioxide (CO_2) and sulfur dioxide (SO_2), which are thought to have promoted global climate change *(11, 12)*. Most authors have argued for global average temperature excursions of ±2°C in relation to these pulses *(7, 8)* (though see ref *(9)* for a contrasting view on such correlations). Under this scenario, this potential kill mechanism either led directly to mass extinction *(5)*, or sufficiently stressed global ecosystems that they become vulnerable to subsequent agents *(13)*. Given that intense and prolonged volcanism appears to be the primary kill mechanism for earlier mass extinctions *(14, 15, 16)*, it is considered by some as the most likely candidate to explain the K/Pg mass extinction *(17)*. However, the timing and size of each eruptive event is highly contentious in relation to the mass extinction event *(8–10)*.

An asteroid, approximately 10 km in diameter, impacted at Chicxulub, in the present-day Gulf of Mexico, 66 Ma (*4, 18, 19)*, leaving a crater ~180–200 km in diameter (Fig. 1a). This impactor struck carbonate and sulfate-rich sediments, leading to the ejection and global dispersal of large quantities of dust, ash, sulfur, and other aerosols into the atmosphere *(4, 18, 19, 20)*. These atmospheric contaminants led to prolonged sunlight screening and global cooling (*19–22),* with severe ecological cascade effects *(4, 13, 23)*. The impact is hypothesized to have precipitated an extremely cold 'impact winter' that was beyond the thermophysiological limits of much of the end-Cretaceous biota *(23)*. A globally ubiquitous ejecta layer *(23)* overlies the latest Cretaceous fossiliferous horizons, marking a biotic change after the K/Pg boundary (Fig. 1a). The size of this impact, its hypothesized global climatic effects, and the worldwide absence of non-avian dinosaurs after it (Fig. 1b), suggest a direct causal relationship between these phenomena *(4, 23)*.

Several modelling approaches have attempted to reproduce the climatic conditions at the K/Pg boundary (*20–22)*, but none has so far quantified the abiotic effect on biological habitability. Herein, we model the climatic conditions at the end-Cretaceous, including the perturbations caused by the two potential extinction drivers. For the first time to our knowledge, we use Habitat suitability modelling to test the effect of these perturbations on the distribution of the dominant Cretaceous terrestrial group, the non-avian dinosaurs.

Results

The climatic perturbations generated by Deccan volcanism (67.4 Ma to 65.5 Ma *(24)*) and the asteroid impact (66.0 Ma *(25)*) are evaluated using coupled Atmosphere-Ocean General Circulation Model (AOGCM; forced by K/Pg boundary conditions) simulations (Fig. 2), which account for the combined effects of aerosol injection (ash, sulphate aerosol and soot deposition affecting surface light reflectance) that cool the climate, with secondary effects such as changes in surface albedo (snow and sea-ice feedback), as well as atmospheric gasses (CO_2) that warm the climate. Ozone concentrations are prescribed at modern-day values. The climate response is calculated using the mean of the last 50 years as well as the 3 years for the peak cooling event in the transient simulations. Climate simulations considered the effect of volcanism, both short-term aerosol injection (tens of years) and long-term CO_2 forcing (hundreds of years) and asteroid impact in isolation (decoupled, excluding long-term concurrent Deccan CO_2 forcing, experiments; Fig. S1–2), and together (coupled, inclusive of Deccan CO_2 forcing, experiments; Fig. S3–6), by means of transient aerosol forcing, where all climatic perturbations evolved with time (Fig. S7). Sensitivity experiments that varied the magnitude of the different perturbations were used to account for variations in the severity of these extreme events (Table S1; Supplementary material).

In the decoupled experiments (Table 1; Table S1), a 5% to 15% solar dimming reduction is considered to simulate the effects of Deccan volcanism or asteroid-induced cooling through reduction in incident SW (shortwave) radiation (-67.9 to -203.6 W/m^2), within the predicted range

of Kaiho et, al. *(18)*. However, the higher end estimate is considered too extreme by some regarding to Deccan, with Schmidt et al. *(16)* suggesting that the reduction in global mean surface temperature from a Deccan magnitude eruption represents no more than a -4.5°C reduction in surface cooling. This is less than the predicted cooling from in the 5% scenario (-9.7°C) suggesting atmospheric cooling as a result of Deccan volcanism will not drive swings in temperature and precipitation that would lead to an extinction level event.

These scenarios only represent a reduction in solar luminosity (in the case of -5% volcanism-induced solar dimming this assumes the best-case scenario [smallest climate forcing] whereby constant volcanic eruption allows replenishment of stratospheric aerosols at the same rate as aerosol loss from the stratosphere) without CO_2 release during 10^2 years of run time. As such, these solar dimming experiments give Deccan volcanism the best possible chance of inflicting an abiotic extinction level event through assuming long-term (1000 years) cooling (decreased solar forcing, mimicking constant aerosol loading of the stratosphere) that is yet to be proven in the rock record *(16)*. Further simulations, with solar luminosity reduced by 10%, 15% and 20% of the end-Cretaceous 'norm', evaluated progressively more extreme asteroid impact scenarios, which have been previously considered to be equivalent *(18, 25)* to a 10–20% lowering of solar input. Two additional simulations assessed the long-term (10^3 years) warming effect caused by Deccan volcanism resulting from increased atmospheric CO_2 release. Both represent extreme scenarios supported by long-term proxy evidence of an increase in atmospheric CO_2 from the 560 ppm baseline in the experiment to (i) 1120 ppm *(26)* and (ii) 1680 ppm *(27, 28)*.

The simulations show that solar dimming (Table 2; Table S2) would have generated global cooling of between 9.7°C to 66.8°C (in the most extreme scenario [20% solar dimming]; Fig. 2b, c; Table 2) on land, but that the addition of CO_2 from Deccan volcanism offset this cooling by warming of +4.7°C to +8.75°C (Fig. 2d, e; Table 2). Multi-proxy reconstructions from Hull, et al. *(10)* have shown a large pulse of Deccan CO_2 release prior to the K/Pg boundary led to only a 2°C warming *(10)*. More precise quantification is difficult because of the uncertain pace and magnitude of Deccan volcanism. Previous work *(26)* highlighted the short residence time of SO_2 in the stratosphere and suggested that the short transient nature (decadal duration) of the eruptions would not have enough long-term effect to force the climate into an extinction state. It has been argued *(16)* that even the 5% solar reduction scenario is an overestimate of the cooling effect of Deccan volcanism, and that a surface temperature cooling of 4.5°C is more likely (half that of the 9.7°C in our 5% solar diming scenario). The solar dimming scenarios would also affect the hydrological cycle. Modelled effects for 5% solar dimming include a 14% decrease and poleward shift in precipitation (Table 2; Fig. S1–3), whereas the most extreme (20%) asteroid-induced solar dimming scenario causes a 95% precipitation decrease.

Transient aerosol experiments (Table 1, 3), at the K/Pg event with and without ash deposition (scenarios 11–14), show a stark cooling (over the 6 year period where stratospheric aerosols are simulated) in global mean temperature (>34°C), followed by a recovery to 'normal', pre-boundary conditions (Fig. 2g–i; Table 3; Fig. S7) over a timeframe of decades. Here, two different transient aerosol-forcing experiments were conducted: (i) the K/Pg impact event based on inferred climate forcing as a result of aerosol release and land surface perturbation (*18, 20–22, 23–25*; Table 3) (with a sensitivity study in which this forcing was reduced by half; Table S3); and (ii) a set of simulations whereby release of CO_2 from Deccan volcanism was included (Table S3). These simulate aerosol loading from the asteroid impact (altering optical depth), as well as increased CO_2 from sustained long-term volcanism, both with simulated volcanogenic aerosol effect (Sc 9–14: Table 1; Fig. 2f, g), and without the latter volcanism-related effects (Sc 7, 8: Table 1; Fig. 2h, i). See Materials and Methods for further details (Supp. Info.). These simulations reproduce an impact that would have generated the same effect as 100 Pinatubo eruptions, hypothesized to be the same impact on climate as the Chicxulub impactor *(30)*. The Pinatubo eruption in 1991 led to the injection of 18–19 Tg of SO_2 into the lower stratosphere, with a 60-fold increase above non-volcanic levels. SO_2 concentrations were still 10x above normal after 2 years' equilibration time (e-folding) of 1 *(30)*. This led to planetary cooling of ~0.5 K and took 7 years for SO_2 to return to pre-eruption levels *(30, 31)*.

After the initial post-impact disturbance of the Cretaceous climate (peak land surface cooling to -34.7°C globally within 5 years; Fig. S7), our transient experiments (Table S3) indicate that the climate system recovery would have taken around 30 years; however, this would have been accelerated by ~10 years with the inclusion of volcanically-derived increased CO_2 (Fig. S7). In this case, the CO_2 would have enabled the climate to recover to 0±5°C within 10 years of the impact, and to pre-impact conditions after ~20 years. An ash layer over North America would have further offset ~4–5°C of land surface cooling, with a small enhancement in recovery to pre-impact temperatures (Fig. S7). The hydrological cycle over land would have been significantly modified, with precipitation reduced by over 85% (Table 3; Fig S1–3) in months after the impact.

Pre-impact end-Cretaceous climate data were used to identify the abiotic conditions favorable for non-avian dinosaurs (Fig. 3a; Methods). This was used as a baseline from which to evaluate the effect of the various modelled climate perturbations (incorporating the relative uncertainties to a suite of modelled climatic scenarios combined with Ensemble modelling *(32)* on the potential global distribution of non-avian dinosaur habitat (Fig. 3a). The 5% solar dimming experiment (Fig. 3b) leads to a disappearance in peak habitability from pre-K/Pg values, with potential habitat reduced to 4% and 24% in lower habitat suitability thresholds (0.5 and 0.3 respectively; Fig. 4). At 10% solar dimming, potential habitat is effectively removed, (0.4% of pre-K/Pg values; Fig. 3c) at the lowest habitability threshold (0.3; Fig. 4). Habitat suitability in solar dimming scenarios is completely extinguished at ≥15% dimming. Global habitability increases in models simulating long-term CO_2 injection due to Deccan volcanism, in case an asteroid impact woul not have happened (Fig. 3d, e): maximum dinosaur habitat suitability increases by ~120% at 1120 ppm of CO_2 and ~97% at 1680 ppm of CO_2. These results suggest that long-term Deccan volcanism alone cannot be responsible for complete dinosaur habitat disruption, without invoking unrealistic volcanic SO_2 forcing (near-constant large ejections) not seen at any point in the Phanerozoic *(16)*. Habitat suitability modelling shows that regions of lower climatically suitable would still be present in more tropical latitudes for dinosaurs in the 5% and, to a lesser degree, in the 10% solar dimming scenarios (forcing too strong according to Schmidt et al. (*16*; Fig. 3). Habitat suitability reaches a critical threshold between the 10% and 15% solar dimming simulations, with no remaining habitat for non-avian dinosaurs in models with 15% dimming (Sc 3, Sc 4, Sc 7, Sc 8; Table 1). Chemical processes are not simulated in these experiments and could further lead to habitat loss.

The transient asteroid experiments show an extinction level event of the non-avian dinosaurs' climatic niche (Fig. 3f, h), coincident with the lowest temperatures reached in experimental simulations after asteroid-induced cooling (Fig. S3c, d). Habitat suitability for these taxa (Table S4) then re-establishes differentially in the models with and without long-term Deccan volcanism CO_2 increase. In scenarios simulating active volcanism (CO_2 increase), at the same time as the impact, maximum habitability increases of 152% from pre-impact levels after recovery (Fig. 3e, G; Fig. 4). In the transient experiments with inactive (no CO_2 release) Deccan volcanism, habitat suitability reaches lower levels than the pre-impact scenario, with 135% more of end-Cretaceous peak habitability once the ecosystem recovers from the impact (~30 years after). It is likely that in both scenarios this would return to pre-impact levels once the climate has fully re-equilibrated. In all transient asteroid impact model experiments for habitat suitability modelling (Table 3), the addition of Deccan-sourced CO_2 (Sc 13–14: Table 1) shows that the short-term transient cooling response is not significantly offset, and that eradication of non-avian dinosaur abiotic niche is pronounced (Fig. 3, 4). On the other hand, recovery rates are accelerated, and post-extinction habitability is re-established at a relatively higher level when coincident volcanism is modelled during the post-impact scenario.

An independent run using MaxEnt *(33, 34)* was performed to test whether these results would corroborate the outcome from the Ensemble simulations (see Methods and Supplementary Material). The 5% solar dimming experiment leads to a substantial, but non-catastrophic, 50% reduction in peak habitability from pre-K/Pg values (Fig. S18a, b). With 10% solar dimming, potential habitat is reduced to 4% of pre-K/Pg values (Fig. S18c), and extinguished at ≥15% dimming. Global habitability is higher in models simulating constant CO_2 injection due to Deccan

volcanism (Fig. S18d, e): maximum dinosaur habitat suitability increases by ~27% at 1120 ppm of CO_2 and ~32% at 1680 ppm of CO_2, confirming the previous Ensemble results in which long-term Deccan volcanism alone cannot be found responsible for complete dinosaur climatic niche extirpation. The simulated transient asteroid impact experiments (Fig. 18f–h) confirm the same trends of the Ensemble outputs (Fig. 3f, h), in providing an almost complete eradication of dinosaur abiotic niche. Even here habitat suitability for these taxa (Table S4) re-establishes more quickly and at higher 'pre-extinction level' when active Deccan volcanism-induced CO_2 injection is simulated as active (122% of pre-impact levels after recovery [Fig. 18e, g; Fig. 19]). Analogously with the Ensemble results, inactive Deccan volcanism fosters a recovery to 92% of end-Cretaceous, pre-impact habitability.

Discussion

The view of Deccan volcanism (both short and/or long term) as the main abiotic driver of the K/Pg mass extinction is often justified by referring to volcanism as a historically strong influencer of global climate *(11, 12)*. Most pertinently, extensive volcanism is recognized as the primary cause behind the most severe biotic crisis of all time, the end-Permian mass extinction, 251 Ma *(35)*, and possibly the Triassic/Jurassic mass extinction, 201 Ma (*15*). However, the timing and duration of the end-Permian extinction was quite different from that of the K/Pg event, with some organisms disappearing earlier than others *(36)* over the course of ~10 myr. The ocean also acidified and became anoxic, which is symptomatic of a geologically slow process *(37–39)*. All of this indicates a prolonged and multiphase extinction process *(35)*. Furthermore, a recent study found no correlation between the timing of Deccan volcanism pulses and global climate changes *(9, 10)* or a large pulse 10^4 prior to the bollide impact questioning Deccan volcanism's influence as an abiotic driver of extinction *(8)*. It is noteworthy that even the stratigraphic inter-beds of the Deccan Traps have yielded dinosaur and other terrestrial fossil remains *(40, 41;* Fig. 1*)*, indicating that animals were able to survive previous high intensity eruptions, even within the epicenter of the Deccan region itself. Given India's geographic isolation at this time, these fossil-bearing beds cannot be explained by biotic restocking via dispersal events *(40)*. Short-term Deccan volcanism (aerosol release), even in the more extreme Deccan-induced 5% solar reduction scenario (with greater sulfur release than hypothesized *(16)* does not perturb the mean climate state sufficiently to produce an inhospitable biosphere globally for non-avian dinosaurs. Even assuming the highest intensity of sulfur injections caused by Deccan volcanism (and longest atmospheric residence times), the order of magnitude of these releases barely approaches the lowest estimates of release by the Chicxulub impactor *(20–22)*. Longrich *(42)* proposed that mammal diversity in latest Cretaceous assemblages (e.g. the North American Hell Creek Formation *(43–45)* actually increases following the Deccan eruption. Given that the hypothisised *(25)* asteroid induced-cooling likely drove the extinction, a pulse of warming (with a similar magnitude as shown in our simulations) *(9)* just prior to the extinction may have actually played as a buffer against cooling induced by the Chicxulub impact, ameliorating the physical effects of bolide impact *(42)*. Such scenario seem to be supported by the recently described continental record of biotic recovery across the K/Pg boundary *(43)*, in which Lyson et al. *(43)* presented stratigraphic and palaeontological evidence of mammalian increase in diversity and body size, coinciding with warming pulses and radiation of major angiosperm clades, and suggesting a possible link with Deccan-induced greenhouse gasses enriching effect.

Even within the site of the asteroid impact, rich communities were re-established within 30 kyr of the K/Pg boundary *(46)*. This implies a very rapid recovery of marine productivity *(46, 47)*, which argues against the suggested delay in ecosystem reset caused by continued Deccan volcanism after the K/Pg boundary *(9, 46, 47)*. In contrast to the end-Permian mass extinction, the K/Pg event was geologically instantaneous *(2–4, 10, 23)*, and there is no clear evidence for a prolonged decline *(3, 4, 48*) that would be required for Deccan volcanism to trigger a mass extinction level event due to the short residence time of stratospheric aerosols. In addition, studies on marine macrofossils from Antarctica are consistent with a sudden, catastrophic driver for the extinction, such as the bolide impact, rather than a significant contribution from Deccan

Traps volcanism during the latest Cretaceous *(49)*. Although some authors have argued for a latest Cretaceous decline in dinosaur diversity, other analytical studies are consistent with relatively high pre-extinction standing diversity, which is compatible with a sudden extinction scenario for non-avian dinosaurs *(48)*. The extinction of only shallow-water marine organisms *(12, 46, 49–51)* highlights a lack of prolonged deep-water acidification, while conjoined isotopic and Earth System Modelling results show rapid oceanic acidification *(50)* and subsequent quick recovery *(50)* compatible with asteroid induced effects in the ocean. One major implication of such a quick event for the marine realm is that the extinction driver must have been in play for a duration shorter than the mixing time of ocean waters (~one thousand years) *(46, 50)*. Our simulations (Tab. 1–2) suggest that sea surface temperatures would have been reduced for all scenarios (Fig. S1, S3, S5, S7), but that the rest of the water-column (>1000 m) was unaffected (Fig. S7b). After the extinction, the marine environment recovered relatively fast, between a few thousand to ~one million years *(9, 46, 47, 50)*.

Whether or not Deccan volcanism actively contributed to temperature decline through atmospheric cooling (via SO_2 aerosol release) is still unclear. The emissions resulting from Deccan volcanism also caused a local atmospheric injection of gas and debris *(24, 28)*, reflecting incident solar radiation from the Sun, but potentially trapping radiant heat in the lower level of the atmosphere *(8, 11, 14)*. It is unclear whether the volatile products from the Deccan reached the stratosphere. With SO_2 stratosphere-residence times being of the order of years, pacing of eruptions would have had to be significant, with sustained high energy activity over 10–100s of years *(16)* to inject a constant supply of climate-cooling aerosols to achieve extinction-driving levels. This rate of volcanism would also have to be at an intensity that would represent a 15–20% reduction in solar luminosity range whose climatic impact is shown to be far beyond that hypothesized *(16)*. Long-term Deccan CO_2 warming would have led to an expansion of dinosaur habitable regions in this study, although the global warming we simulate is slightly higher than suggested by proxy-records (~3°C in scenario 5 as opposed to ~2°C *(10)*. A longer-term effect of volcanism would directly (and potentially indirectly through a weakened alkalinity pump *(50)*) increase CO_2 content offsetting individual short-term cooling events and increasing habitability.

We show that the abiotic impact of Deccan volcanism was not sufficient to cause the extinction of non-avian dinosaurs, while the effects of the impact alone were enough to cause the extinction. It is more likely that the Deccan's influence after the event might have been of greater importance in determining ecological recovery rates after the asteroid-induced cooling, rather than delaying it *(43)*. This also fits well with a recent recalibration that suggests that much of the heightened volcanic activity occurred after the K/Pg boundary *(9, 10)*.

The lithology of the target rocks collided by the Chicxulub asteroid led to a massive release of hundreds of Gt of sulfates *(21, 22, 29)*, yet it is unknown how much reached the stratosphere *(16)*, with a correlated cooling effect of 27° C (22). This would have led to 3 to 16 years of sub-freezing temperatures and a recovery time of more than 30 years. Results from the most recent IODP drilling expedition *(29)* suggest that the estimate of sulfur injected to the atmosphere by the impact should be much higher (325 ± 130 Gt of sulfur and 425 ± 160 Gt of CO_2), which might have generated cooling for centuries *(37)*. Clearly, the asteroid impact was devastating to Earth's climate, leading to freezing temperatures on land (simulated duration in herein reported experiments of ~30 years), even at the tropics, disrupting large faunal food supply and destabilising all trophic levels.

Non-avian dinosaurs were not the only victims of the K/Pg mass extinction. Other vertebrate taxa, such as birds *(52, 53)*, mammals *(54, 42)*, and squamates *(55, 56)*, were affected by severe extinction rates *(57)*, whereas other groups, such as crocodylomorphs, turtles, and choristoderes were affected to a lesser degree *(57–60)*. Without even accounting for other terrestrial and marine animals affected (or completely wiped out, *(1, 61, 62)*, it appears that organisms from a vast array of different ecologies were hit by the extinction mechanism. An ecological determinant behind the high selectivity of the process may be found in variables like body size, diet, physiology, habitat, and geographic range *(5, 57, 63)*. Many of these ecological traits can be, to a certain degree, linked to temperature fluctuations. We know for example that habitat, body size, and geographic ranges in living members of crown group Archosauria are extremely sensitive to

thermal excursions *(63–65)*. Ecosystem structure can also be severely affected by drastic temperature variations, with an important impact on biodiversity *(66, 67),* as it has already been suggested for the K/Pg mass extinction *(13)*. An ecological refugium-role, potentially offered by the higher thermal inertia of freshwater environments, microhabitats, or the trophic opportunities provided by the detritus cycle *(57, 68)*, may be a potential explanation behind this differential survivorship process. Refugia from extinction level temperature excursion might have been found in deep valleys, fluvio-lacustrine systems, coastal regions, and in the tropics, which would have offered shelter for taxa such as birds, mammals, turtles, crocodiles, lizards, and snakes, all of which survived the K-Pg mass extinction with comparatively little species loss *(42, 43, 45, 53, 55)*. Lowered biotic barriers *(69)* coinciding with warming pulses (*9*) that sped-up the thermic recovery of Earth System, might have boosted an ecological recovery and consequent release across the boundary in the earliest Danian *(10, 42, 43)*.

These elements imply a cause-effect relationship between the Chicxulub impactor and the K/Pg mass extinction of non-avian dinosaurs. Furthermore, GCMs and habitat suitability modelling simulations suggest that climatically active volcanic by-products might have sped up recovery after an impact winter-induced mass extinction. If this is the case, the perception of Deccan volcanism as a K/Pg extinction driver might need to shift to a new paradigm which emphasizes the mitigating effect that volcanism could have had on global cooling. Our results support the Alvarez hypothesis *(23)*, which attributes the end-Cretaceous mass extinction to a prolonged impact winter, as the most likely explanation for the extinction of non-avian dinosaurs. Although we do not discount the impact from biotic effects or other, not tested here, abiotic drivers (e.g. wildfire, acid rain), these results show that even without them the impact winter would have led to dinosaur demise. We demonstrate possible climatological threshold necessary to trigger the complete extinction of non-avian dinosaurs. Furthermore, we suggest that Deccan volcanism might have contributed to the survival of many species across the K/Pg boundary, and potentially fostered the rapid recovery of life from the most iconic of mass extinctions. This modeling approach has the potential to be used for clades (where sampling is spatially and temporally abundant and robust) to de-convolve the impact of secular climate change as a result of various abiotic forcings.

Although we focus on a more likely terrestrial asteroid impact *(18)* it has been suggested that a deep ocean impact that does not reach the bathymetric surface could result in a substantial injection of water vapour into the stratosphere. It has been suggested that in such a scenario that increased oceanic derived stratospheric water vapour may have cancelled out any aerosol cooling effect and led to significant surface warming *(70)*. Future studies should focus on investigating the effect of other abiotic drivers (e.g. acidification, halogens, significant surface warming, UV radiation, fire, carbon cycle disruption) of both asteroid impact and Deccan volcanism, as this may offer another avenue to understand the relative effect of both events.

Materials and Methods

General circulation models of end-Cretaceous extinction scenarios

The climate simulations were carried out using the coupled Atmosphere-Ocean General Circulation Model (AOGCM), HadCM3L-M2.1 *(71)*). HadCM3L has contributed to the Coupled Mode Intercomparison Project (CMIP) experiments demonstrating skill at reproducing the modern day climate *(71, 72)* and has been used for an array of different paleoclimate experiments *(73–75).* Unlike previous studies using AOGCMs *(18*, *76–78)* to explor the effect of end-Cretaceous volcanism and asteroid impact (and associated aerosol ejecta) we do not use a modern-day topography and bathymetry, but a geologic stage specific boundary conditions representative of the end-Cretaceous palaeogeography instead *(6)*. Carbon dioxide concentrations at the end-Cretaceous were set to 560 ppm, within the range of recent pCO_2 reconstructions *(79, 80)*.

The simulations of the extinction scenarios (Table S1) are separated into their (1a) short-term and (1b) long-term impact on climate and ultimately non-avian dinosaur abiotic niche. The simulation of Deccan volcanism scenarios is obtained by perturbing the climate by either: 2a -

sustained stratospheric sulfate aerosol loading, or 2b - sustained increased CO_2. Because of uncertainty in the amount of aerosol release from such events, we investigate the impact of volcanism as a function of a constant reduction in solar radiation (solar dimming) at the Earth's surface simulating the radiative cooling effect of sulphate aerosols in the stratosphere. A reduction in solar radiation equal to 5-15% has been hypothesized to be comparable for Deccan volcanism (without CO_2 release) *(24, 79–81)*. To test uncertainty of Deccan volcanism stratospheric aerosol loading and associated cooling we also test the impact of 15-20% solar reduction, which can also be used synonymously as an asteroid impact solar luminosity reduction analogue due to predicted change in radiative forcing *(25)*.

Sustained volcanic release of CO_2 has been hypothesized *(81– 84)* as a potential mechanism of extinction in the end Cretaceous. Two idealized large injections of CO_2 have been simulated over a 200-year period. Both represent extremes scenarios supported by geological evidence of an increase in CO_2 from the 560 ppm baseline CO_2 in the model to i) 1120 ppm *(26)* and ii) 1680 ppm *(16, 27)* CO_2. Previous attempts in constraining the total volume of eruptive material and volatiles *(26)* refer to a CO_2 release of ×2.1–4 times, so that our ×4CO_2 scenario models an extreme Deccan release. Numerical values for the physical parameters in the decoupled (Table S2), and transient coupled (Table S3) are reported.

We prescribe stratospheric sulphate aerosol concentrations as a function of the impact on atmospheric optical depth to simulate an extraterrestrial asteroid impact. Optical depths at 0.55μm were taken from observations *(27)* of the 1991 Pinatubo eruption with sulphate aerosol loading of the stratosphere equivalent to 100 times the forcing of the Pinatubo eruption *(27, 20)* consistent with the estimates of Pierazzo, et al. *(20).* The radiative impact of sulphate aerosols is simulated through absorbing and scattering incoming solar radiation across a spectral range of 0.2–10 μm assuming a constant aerosol size distribution *(85)*. A Stratospheric residence time of ~6 years for the sulphate aerosol was implemented taking into account the longer hypothesized residence time of Pierazzo *(20–22)* due to increased atmospheric stratification as a result of concurrent surface cooling and stratospheric warming *(86).* Stratospheric injection of aerosols into the model was initialized at year 40 into the 200-year simulation. Outside of this 6-year asteroid impact aerosol injection window, no aerosols were released as there is no known baseline aerosol concentration for the Maastrichtian time period to apply. To test the sensitivity of the 100× Pinatubo forcing, we also simulate the impact of a less severe asteroid impact with a 50× Pinatubo set of simulations. The individual impacts of increased CO_2, ash layer, and a 100× and 50× Pinatubo aerosol forcing were also simulated. Explanations for all simulations are listed in Table S1.

Episodic eruptions over the last 350 kyr of the Cretaceous would have increased the amount of CO_2 in the atmosphere and so we also consider a set of simulations with and without the impact of CO_2 degassing as a result of Deccan volcanism (Table S2). CO_2 will have the competing effect of increasing global temperature potentially offsetting the impact of cooling from stratospheric sulfate aerosols. The precise amount of CO_2 released from Deccan volcanism is unknown due to the difficulty in constraining the total volume of eruptive material and volatiles *(24)*. Here we use a conservative approach by doubling the baseline CO_2 concentration at the start of the simulation. This is greater than predicted for even the most extreme scenarios *(24, 87)*. Although the amount is likely unrealistic, this does evaluate the potential of volcanically derived CO_2 to mitigate for the cooling effects of impact-derived SO_2.

A set of simulations with and without a continental size ash blanket *(88)* over North America (latitudes 67.5°N to 15°N and longitudes 26.25°W to 116.25°W) that may have occurred from the fallout are also performed. For simplicity and due to the uncertainty in the longevity of the ash layer we prescribed the ash layer for the duration of the 200-year simulation. For the composition of the imposed ash layer and soil properties from observations we follow Jones, et al. *(88)*.

A reduction in solar radiation of -5%, -10%, -15% and -20% of Maastrichtian solar luminosity is reproduced for increasingly more extreme asteroid impact scenarios (a solar dimming between 10–20% has been discussed in published estimates for atmospheric radiative transfer models of sunlight filtration at the K/Pg event) *(24, 25)*. These are obtained by reducing solar luminosity by

5%, 10%, 15% and 20% for a 200-year period under 2xCO_2 conditions (Table S2). This allows a range of hypothesized impact events simulating the effect of different potential magnitudes. See supplementary material for expanded discussion and figures on baseline boundary conditions and simulation of the different extinction scenarios.

Dinosaur occurrence dataset

The fossil occurrence dataset was assembled by downloading a comprehensive database of late Maastrichtian (69–66 Ma) global dinosaur fossil occurrences from the Paleobiology Database (PaleobioDB: https://paleobiodb.org) on 6th April 2018 (Supplementary Data S1-2) which have been properly checked for accuracy and cleaned to obtain a dataset of 2088 entries. These occurrences belong to 9 clades of the end-Cretaceous global dinosaurian fauna *(76)* and comprise the: Ankylosauria, Ceratopsidae, Deinonychosauria, Hadrosauridae, Ornithomimosauria, Oviraptorosauria, Pachycephalosauridae, Sauropoda and Tyrannosauridae. Expanded discussion on spatial occurrences preparation is reported in the Supplementary Material.

Habitat suitability modelling

GCM-derived environmental variables were chosen based on broad autecological analogy with their most closely related living organisms ([crocodiles + birds *(89–91)*]). We used Pearson's pairwise correlation test to determine co-linearity between variables (Fig. S8), keeping only the predictors showing a Pearson's correlation coefficient below 0.7 to prevent overfitting. The climatic variables used for our habitat suitability modelling (HSM) were the temperatures of the warmest and coldest annual quartiles and the precipitation of the wettest and driest yearly quarters (Fig. S9–17). These analyses were run in R version 3.5.1 (R core team 2018) with the biomod2 package *(92, 93)* for Ensemble modelling *(32)* and using MaxEnt (maximum entropy algorithm *(33, 34)*) in the java platform version 3.4.1.

All raw data (environmental variables and occurrence data) and modelling outputs are reported in the Supplementary material of this article (Data S1–14).

Expanded discussion on HSM and figures on additional HSMs are presented in supplementary material, with all settings from Ensemble and MaxEnt modelling reported. The scripts for habitat suitability quantification in areal extent are reported in Data S13-S14.

Acknowledgments

We are grateful for the efforts of all those who have generated Maastrichtian dinosaur fossil data, as well as those who have entered these data into the Paleobiology Database, especially Matthew Carrano and John Alroy. We thank Getech, PLC. for providing palaeogeographic base maps, digital elevation models and palaeorotation of fossil occurrences used in this study. Lewis Jones (Imperial College London) is thanked for relevant discussions on habitat suitability modelling. Jack Mayer Wood is thanked for the dinosaur silhouette reported in Figure 1 and used under CC BY 3.0 license (https://creativecommons.org/licenses/by/3.0/ CC BY 3.0). Christopher Dean (University of Birmingham) is acknowledged for scientific discussion relevant to this study. A.A.C. was supported by an Imperial College London Janet Watson Departmental PhD Scholarship, A.F. and D.J.L. acknowledge NERC grant NE/K014757/1, Cretaceous-Paleocene-Eocene: Exploring Climate and Climate Sensitivity, P.D.M. was supported by a Royal Society University Research Fellowship (UF160216).

References

1. D. M. Raup, J. J., Jr. Sepkoski, Mass extinctions in the marine fossil record: Science, 215, 1501-1503 (1982).
2. D. E. Fastovsky, P. M. Sheehan, The extinction of the dinosaurs in North America. GSA Today 15, 4 (2005).
3. A. A. Chiarenza et al. Ecological niche modelling does not support climatically-driven dinosaur diversity decline before the Cretaceous/Paleogene mass extinction. Nat. Commun. 10, 1091 (2019).
4. P. Schulte et al. The Chicxulub asteroid impact and mass extinction at the Cretaceous-Paleogene boundary. Science, 327, 1214–1218 (2010).
5. J. D. Archibald et al. Cretaceous extinctions: multiple causes. Science, 328, 973 (2010).
6. A. Farnsworth et al. Climate sensitivity on geological timescales controlled by nonlinear feedbacks and ocean circulation. Geophy. Res. Lett., 46, 9880–9889 (2019).
7. V. E. Courtillot, P. R. Renne, Sur l'âge des trapps basaltiques (On the ages of flood basalt events). Comptes Rendus Geosc., 335, 113–140 (2003).
8. B. Shoene, et al. U-Pb constraints on pulsed eruption of the Deccan Traps across the end-Cretaceous mass extinction. Science, 363, 862–866 (2019).
9. C. J. Sprain et al. The eruptive tempo of Deccan volcanism in relation to the Cretaceous-Paleogene boundary. Science, 363, 866–870 (2019).
10. P. M. Hull et al. On impact and volcanism across the Cretaceous-Paleogene boundary. Science 367(6475): 266-272 (2020). doi: 10.1126/science.aay5055
11. D. L. Royer et al. CO2 as a primary driver of Phanerozoic climate. GSA Today. 14: 4–10 (2004). doi:10.1130/1052-5173
12. P. Wilf, K. R. Johnson, B. T. Huber, Correlated terrestrial and marine evidence for global climate changes before mass extinction at the Cretaceous-Paleogene boundary. Proc. Natl. Acad. Sci. U.S.A. 100, 599 (2003). doi:10.1073/pnas.0234701100
13. J. S Mitchell et al., Late Cretaceous restructuring of terrestrial communities facilitated the end-Cretaceous mass extinction in North America. Proc. Natl. Acad. Sci. U.S.A. 109, 18857–18861 (2012).
14. P. R. Renne et al. Time scales of critical events around the Cretaceous-Paleogene boundary. Science, 339, 684 (2013); doi: 10.1126/science.1230492.
15. D. P.G. Bond, P. B. Wignall. Large igneous provinces and mass extinctions: An update", Volcanism, Impacts, and Mass Extinctions: Causes and Effects, Gerta Keller, Andrew C. Kerr. GSA Special Papers, 505, doi: 10.1130/SPE505 (2014).
16. A. Schmidt et al., Selective environmental stress from sulphur emitted by continental flood basalt eruptions. Nat Geosci 9, 77-82 (2016).
17. E. Font et al. Deccan volcanism induced high-stress environment during the Cretaceous–Paleogene transition at Zumaia, Spain: Evidence from magnetic, mineralogical and biostratigraphic records. Earth and Planetary Science Letters. 484, 53-66 (2018). DOI: 10.1016/j.epsl.2017.11.055.
18. K. Kaiho et al., Global climate change driven by soot at the K-Pg boundary as the cause of the mass extinction. Sci Rep-Uk 6, (2016).
19. J. Vellekoop. et al. Rapid short-term cooling following the Chicxulub impact at the Cretaceous–Paleogene boundary. Proc. Natl. Acad. Sci. USA 111, 7537-7541 (2014).
20. E. Pierazzo, A. N. Hahmann, L. C. Sloan, Chicxulub and climate: Radiative perturbations of impact-produced S-bearing gases. Astrobiology 3, 99 (2003). doi:10.1089/153110703321632453
21. J. Brugger, G. Feulner, S. Petri, Baby, it's cold outside: Climate model simulations of the effects of the asteroid impact at the end of the Cretaceous, Geophys. Res. Lett., 44, 419–427 (2017). doi: 10.1002/2016GL072241.
22. K. O. Pope, K. H. Baines, A. C. Ocampo, B. A. Ivanov, Energy, volatile production, and climatic effects of the Chicxulub Cretaceous/Tertiary impact. J. Geophys. Res. 102, (E9), 21645 (1997). doi:10.1029/97JE01743

23. L. W. Alvarez, W. Alvarez, F. Asaro, H. V. Michel, Extraterrestrial cause for the Cretaceous-Tertiary extinction. Science 208, 1095 (1980). doi:10.1126/science.208.4448.1095
24. A.-L. Chenet et al., Determination of rapid Deccan eruptions across the Cretaceous-Tertiary boundary using paleomagnetic secular variation: 2. Constraints from analysis of eight new sections and synthesis for a 3500-m-thick composite section. J. Geophys. Res. 114, (B6), B06103 (2009). doi:10.1029/2008JB005644X.
25. K. Pope, K. Baines K, Ocampo A, Ivanov B. Impact winter and the Cretaceous/Tertiary extinctions: Results of a Chicxulub asteroid impact model, Earth and Planetary Science Letters 128, 719-725 (1994).
26. T. S. Tobin, C. M. Bitz, D. Archer, Modeling climatic effects of carbon dioxide emissions from Deccan Traps volcanic eruptions around the Cretaceous-Paleogene boundary. Palaeogeogr Palaeocl 478, 139-148 (2017).
27. M. Sato, J. E. Hansen, M. P. Mccormick, J. B. Pollack, Stratospheric Aerosol Optical Depths, 1850-1990. J Geophys Res-Atmos 98, 22987-22994 (1993).
28. S. Self, M. Widdowson, T. Thordarson, A. E. Jay, Volatile fluxes during flood basalt eruptions and potential effects on the global environment: A Deccan perspective. Earth Planet. Sci. Lett. 248, 518 (2006). doi:10.1016/j.epsl.2006.05.041
29. N. Artemieva, J. Morgan, & Expedition 364 Science Party. Quantifying the release of climate-active gases by large meteorite impacts with a case study of Chicxulub. Geoph. Res. Lett., 44, (10) 180–10, 188 (2017). doi.org/10.1002/2017GL074879
30. B. J. Soden et al. Global Cooling After the Eruption of Mount Pinatubo: A Test of Climate Feedback by Water Vapor. Science, 296, (5568) 727–730 (2002).
31. S. Kremser et al., Stratospheric aerosol—Observations, processes, and impact on climate. Reviews of Geophysics, 54, 278–335 (2016). https://doi.org/10.1002/2015RG000511
32. M. B. Araújo et al. Standards for distribution models in biodiversity assessments. Science Advances 5, eaat4858 (2019).
33. S. J. Phillips et al. Opening the black box: an open-source release of Maxent. Ecography. 40 (7), 887–893 (2017).
34. J. Elith et al. A statistical explanation of MaxEnt for ecologists. Divers. Distrib. 17, 43–57 (2011).
35. M. W. Broadley, et al. End-Permian extinction amplified by plume-induced release of recycled lithospheric volatiles. Nature Geoscience, 11, 682–687 (2018). doi: 10.1038/s41561-018-0215-4
36. S. Sahney, M. J Benton, Recovery from the most profound mass extinction of all time. Proc. of the R. Soc. B, 275 (1636): 759–765 (2008). doi:10.1098/rspb.2007.1370.
37. P. Shulte et al., Response—Cretaceous Extinctions. Science, 328, (5981) 975–976. doi: 10.1126/science.328.5981.975
38. P. B. Wignall, Large igneous provinces and mass extinctions, Earth Science Reviews, 53, 1–33 (2001). doi: 10.1016/S0012-8252(00)00037-4.
39. R.V. White, A.D. Saunders. Volcanism, impact and mass extinctions: incredible or credible coincidences? Lithos, 79, 299–316 (2005).
40. V. V. Kapur et al. Paleoenvironmental and paleobiogeographical implications of the microfossil assemblage from the Late Cretaceous intertrappean beds of the Manawar area, District Dhar, Madhya Pradesh, Central India. Historical Biology, 31:9, 1145-1160 (2018). Doi: 10.1080/08912963.2018.1425408
41. V. R. Guntupalli and A. S. Prasad, Vertebrate fauna from the Deccan volcanic province: Response to volcanic activity. In Volcanism, Impacts, and Mass Extinctions: Causes and Effects, Gerta Keller, Andrew C. Kerr (2014).
42. N. R. Longrich et al. Severe extinction and rapid recovery of mammals across the Cretaceous–Palaeogene boundary, and the effects of rarity on patterns of extinction and recovery. J. Evol. Biol., 29: 1495-1512 (2016). doi:10.1111/jeb.12882

43. T. R. Lyson et al. Exceptional continental record of biotic recovery after the Cretaceous–Paleogene mass extinction, Science, 977-983 (2019).
44. G.P. Wilson. Mammalian faunal dynamics during the last 1.8 million years of the Cretaceous in Garfield County, Montana. J. Mamm. Evol. 12: 53–76 (2005).
45. G.P. Wilson. Mammalian extinction, survival, and recovery dynamics across the Cretaceous-Paleogene boundary in northeastern Montana, USA. Geol. Soc. Am. Spec. Pap. 503: 365–392 (2014).
46. C. M. Lowery et al., Rapid recovery of life at ground zero of the End-Cretaceous mass extinction, Nature, 558, 288–291 (2018). doi:10.1038/s41586-018-0163-6.
47. B. Schaefer et al. Microbial life in the nascent Chicxulub crater. Geology (2020). doi: https://doi.org/10.1130/G46799.1
48. S. L. Brusatte et al. The extinction of the dinosaurs. Biol. Rev. 90, 628–642 (2015).
49. J. D. Witts et al. Macrofossil evidence for a rapid and severe Cretaceous–Paleogene mass extinction in Antarctica, Nat. Commun. (2016). doi: 10.1038/NCOMMS11738
50. M. J. Henehan et al. Rapid ocean acidification and protracted Earth system recovery followed the end-Cretaceous Chicxulub impact. PNAS, 116 (45) 22500-22504 (2019). Doi: 10.1073/pnas.1905989116.
51. J. Vellekoopet al. Type-Maastrichtian gastropod faunas show rapid ecosystem recovery following the Cretaceous–Palaeogene boundary catastrophe. Palaeontology. doi:10.1111/pala.12462 (2019).
52. D.J. Field et al. Early evolution of modern birds structured by global forest collapse at the end-Cretaceous mass extinction. Current Biology, 28: 1-7 (2018). https://doi.org/10.1016/j.cub.2018.04.062
53. N. R. Longrich et al. Mass extinction of birds at the Cretaceous-Paleogene (K-Pg) boundary. PNAS, 108(37):15253-7 (2011).
54. T. Halliday et al. Eutherians experienced elevated evolutionary rates in the immediate aftermath of the Cretaceous–Palaeogene mass extinction. Proc. R. Soc. B., 283, 20153026. (2016) doi: 10.1098/rspb.2015.3026
55. T. J. Cleary et al. Lepidosaurian diversity in the Mesozoic–Palaeogene: the potential roles of sampling biases and environmental drivers. Proc. R. Soc. Lond. B. (2018). doi: 10.1098/rsos.171830
56. N. R. Longrich et al. Mass extinction of lizards and snakes at the Cretaceous-Paleogene boundary. PNAS. 109(52):21396-401 (2012).
57. P. M. Sheehan, D. E. Fastovsky 1992. Major extinctions of land-dwelling vertebrates at the Cretaceous-Tertiary boundary, Eastern Montana. Geology, (1992) 20:556-60.
58. J. D. Archibald, J. J. Bryant. Differential Cretaceous–Tertiary extinction of nonmarine vertebrates; evidence from northeastern Montana. In: Sharpton VL, Ward PD, editors. Global catastrophes in earth history: An interdisciplinary conference on impacts, volcanism, and mass mortality. GSA Special Paper, 247:549-62 (1990).
59. M. J. Benton. Mass extinctions among tetrapods and the quality of the fossil record. Proc. R. Soc. Lond. B. 325:369–386 (1990).
60. L. J. Bryant. Non-dinosaurian lower vertebrates across the Cretaceous-Tertiary boundary in northeastern Montana. University of California Publications in Geological Sciences. 134:1-107 (1989)
61. J. Sepkoski. A Compendium of Fossil Marine Animal Genera, Bull. of Am. Paleontol., vol. 363, edited by D. Jablonski , M. Foote, Paleontol. Res. Inst., Ithaca, N. Y (2002).
62. R. B. J. Benson, R. J. Butler. Uncovering the diversification history of marine tetrapods: ecology influences the effect of geological sampling biases.Geol. Soc. Lond. Spec. Publ. 358: 191-208 (2011).
63. F. J. Mazzotti et al. Large reptiles and cold temperatures: do extreme cold spells set distributional limits for tropical reptiles in Florida? Ecosphere, 7(8):e01439 (2016). 10.1002/ecs2.1439
64. G. C. Grigg et al. Thermal relations of very large crocodiles, Crocodylus porosus, free-ranging in a naturalistic situation. Proc. R. Soc. Lond. B. 265, 1793 -1799 (1998).

65. Andrew et al. Clinal variation in avian body size is better explained by summer maximum temperatures during development than by cold winter temperatures. The Auk: Ornithological Advances (2018). doi: 10.1642/AUK-17-129.1
66. N. B. Grimm et al. 2013. The impacts of climate change on ecosystem structure and function. Frontiers in Ecology and the Environment, 11: 474-482. doi:10.1890/120282
67. F. C. Garcia et al. Changes in temperature alter the relationship between biodiversity and ecosystem functioning. PNAS, 115 (43) 10989-10994 (2018); doi: 10.1073/pnas.1805518115
68. M. O'Leary et al. The placental mammal ancestor and the Post-K–Pg radiation of placentals. Science 339, 662–667 (2013).
69. N. R. Longrich et al. Biogeography of worm lizards (Amphisbaenia) driven by end-Cretaceous mass extinction. Proc. R. Soc. Lond. B Biol. Sci. 202: 20143034 (2015).
70. M. Joshi et al. Global warming and ocean stratification: A potential result of large extraterrestrial impacts, Geophys. Res. Lett. 44, 3841– 3848 (2017). doi:10.1002/2017GL073330
71. P. J. Valdes et al., The BRIDGE HadCM3 family of climate models: HadCM3@Bristol v1.0. Geosci Model Dev 10, 3715-3743 (2017).
72. M. Collins, S. F. B. Tett, C. Cooper, The internal climate variability of HadCM3, a version of the Hadley Centre coupled model without flux adjustments. Clim Dynam 17, 61-81 (2001).
73. D. J. Lunt et al., Palaeogeographic controls on climate and proxy interpretation. Clim Past 12, 1181-1198 (2016).
74. A. Marzocchi et al., Orbital control on late Miocene climate and the North African monsoon: insight from an ensemble of sub-precessional simulations. Clim Past 11, 1271-1295 (2015).
75. A. T. Kennedy, A. Farnsworth, D. J. Lunt, C. H. Lear, P. J. Markwick, Atmospheric and oceanic impacts of Antarctic glaciation across the Eocene-Oligocene transition. Philos. T. R. Soc. A 373, (2015).
76. D. J. Beerling, A. Fox, D. S. Stevenson, P. J. Valdes, Enhanced chemistry-climate feedbacks in past greenhouse worlds. P Natl Acad Sci USA 108, 9770-9775 (2011).
77. C. G. Bardeen, R. R. Garcia, O. B. Toon, A. J. Conley, On transient climate change at the Cretaceous-Paleogene boundary due to atmospheric soot injections. P Natl Acad Sci USA 114, E7415-E7424 (2017).
78. C. Covey, S. L. Thompson, P. R. Weissman, M. C. Maccracken, Global Climatic Effects of Atmospheric Dust from an Asteroid or Comet Impact on Earth. Global and Planetary Change 9, 263-273 (1994).
79. D. L. Royer, M. Pagani, D. J. Beerling, Geobiological constraints on Earth system sensitivity to CO2 during the Cretaceous and Cenozoic. Geobiology 10, 298-310 (2012).
80. G. L. Foster, D. L. Royer, D. J. Lunt, Future climate forcing potentially without precedent in the last 420 million years. Nat Commun 8, (2017).
81. S. Bekki et al., The role of microphysical and chemical processes in prolonging the climate forcing of the Toba eruption. Geophys. Res. Lett. 23, 2669-2672 (1996).
82. D. J. Beerling et al., An atmospheric pCO2 reconstruction across the Cretaceous-Tertiary boundary from leaf megafossils. PNAS, 99 (12) 7836-7840 (2002).
83. J. D. O'Keefe, T. J. Ahrens. Impact production of CO2 by the Cretaceous/Tertiary extinction bolide and the resultant heating of the Earth. Nature, 338, 247–249 (1989).
84. K. J. Hsü et al., Mass mortality and its environmental and evolutionary consequences. Science, 216, 249-256 (1982).
85. D. A. Kring and D. D. Durda, Trajectories and distribution of material ejected from the Chicxulub impact crater: Implications for postimpact wildfires. J. Geophys. Res. 107, E8 (2002).
86. M. Joshi et al., Global warming and ocean stratification: A potential result of large extraterrestrial impacts. Geophys. Res. Lett., 44, 3841– 3848 (2017).

87. M. Mussard et al, Modeling the carbon-sulfate interplays in climate changes related to the emplacement of continental flood basalts. Geol. Soc. Am. Spec. Pap. 505, 339–352. (2014).
88. M. T. Jones, R. S. J. Sparks, P. J. Valdes, The climatic impact of supervolcanic ash blankets. Clim Dynam 29, 553-564 (2007).
89. A. Guisan, U. Hofer, Predicting reptile distributions at the mesoscale: relation to climate and topography. J. of Biogeog. 30, 1233–1243 (2003).
90. A. T. Peterson, Predicting species' geographic distributions based on ecological niche modeling. Condor, 103, 599–605 (2001).
91. A. T. Peterson, L. F. Ball, K. P. Cohoon. Predicting distributions of Mexican birds using ecological niche modelling methods. Ibis, 144, E27–E32 (2002).
92. W. Thuiller, D. Georges, R. Engler, biomod2: Ensemble platform for species distribution modeling. R package version 3.1-64 (2014).
93. W. Thuiller, B. Lafourcade, R. Engler, M. B. Araujo, BIOMOD – A platform for ensemble forecasting of species distributions. Ecography, 32, 369-373 (2009).

Figures and Tables

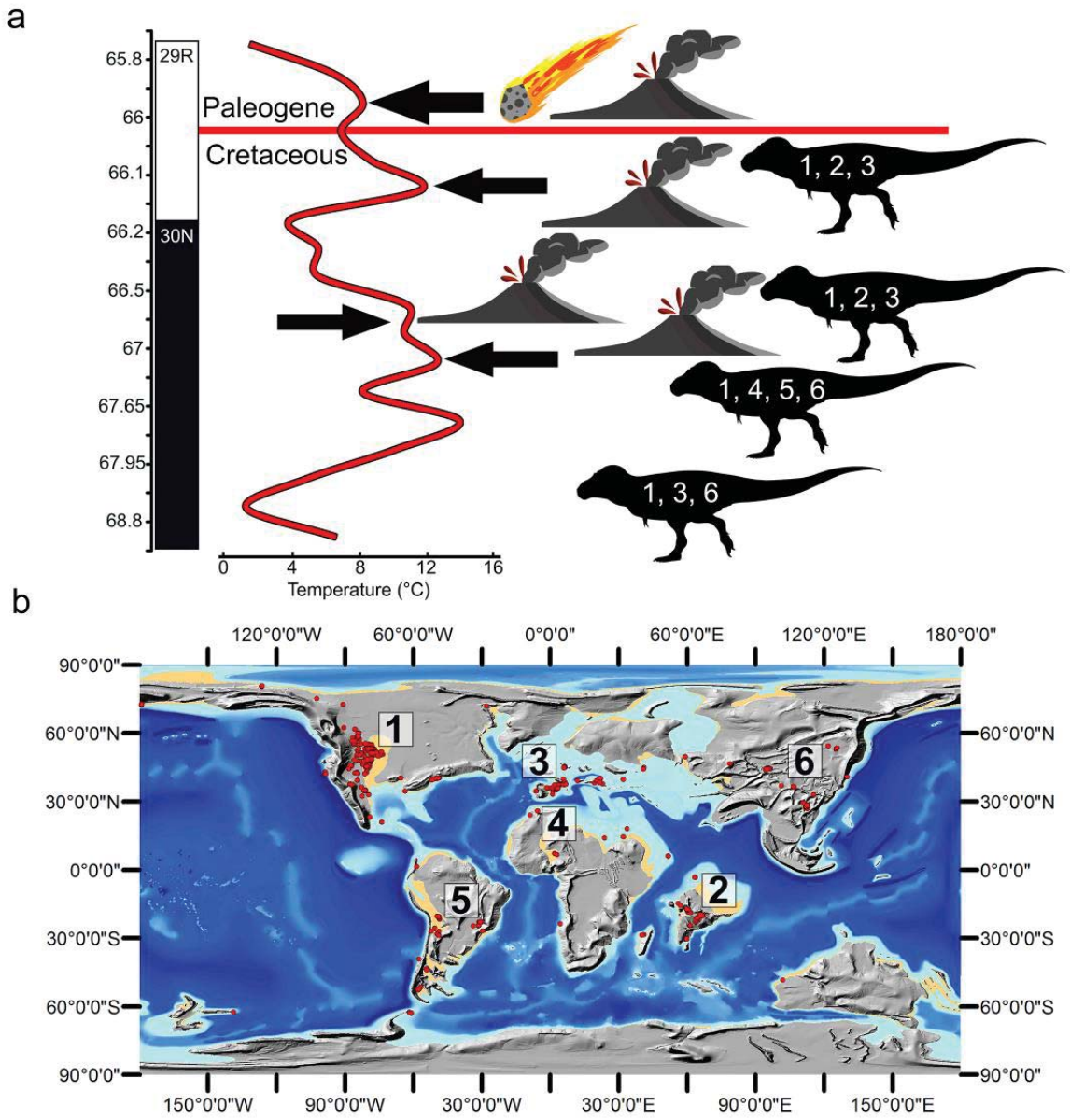

Figure 1. Geologic (a) and paleontological (b) records of the K/Pg mass extinction. Paleothermometer (a) showing the Deccan induced warming with the two main episodes of volcanism highlighted by the black arrows and symbols of volcanoes. The last phase endures the end of the Cretaceous, characterized by the bolide impact in Chicxulub. Fossil remains of non-avian dinosaurs (both body fossils, egg fragments and nesting sites) occur throughout the whole stratigraphic record of prolonged volcanism episodes (dinosaur silhouettes). Numbers in a represent Upper Maastrichtian dinosaur bearing localities, mapped on a Late Maastrichtian palaeogeography in B. 1, Hell Creek formation (USA); 2, Lameta formation (India); 3, Tremp Formation; 4, Couche III formation (Morocco); 5, Marilía formation (Brazil); 6, Nemegt formation (Mongolia).

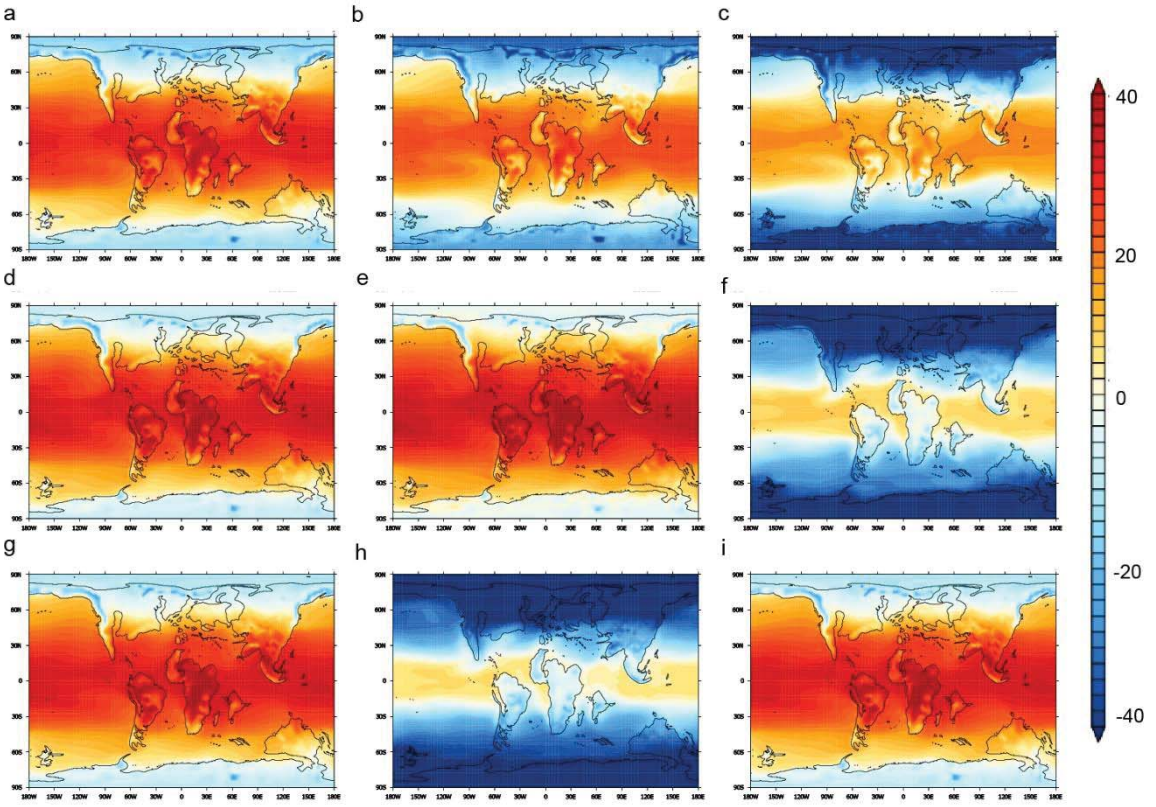

Figure 2. K/Pg Surface temperature (°C) outputs from General Circulation Models (GCMs). Heat maps represent temperature fluctuations from the late Maastrichtian control, with cooler temperatures in blue and warmer in red. Late Maastrichtian climate control (a) is perturbed in (b) by a solar dimming simulation reproducing the effect of mild asteroid impact or extreme volcanism-induced cooling (b) at 5% (Sc 1) and of a more extreme asteroid-induced cooling scenario (c) at 10% (Sc 2) of solar radiation reduction. The effect of prolonged volcanism is reproduced with an increase to 1120 ppm of (d) CO_2 content (Sc 5) and to (e) 1680 ppm of CO_2 (Sc 6). A transient model including both Deccan volcanism and the effect of the Chicxulub impact is shown in F (Sc 11) and G (Sc 12), and with inactive volcanism (H, Sc 13 and I, Sc 14), while the 3 coldest years of the impact are modelled in F (Sc 11) and H (Sc 13; additional details and figures on GCMs are in Supplementary material). Temperature scale running from -40 to 40 °C.

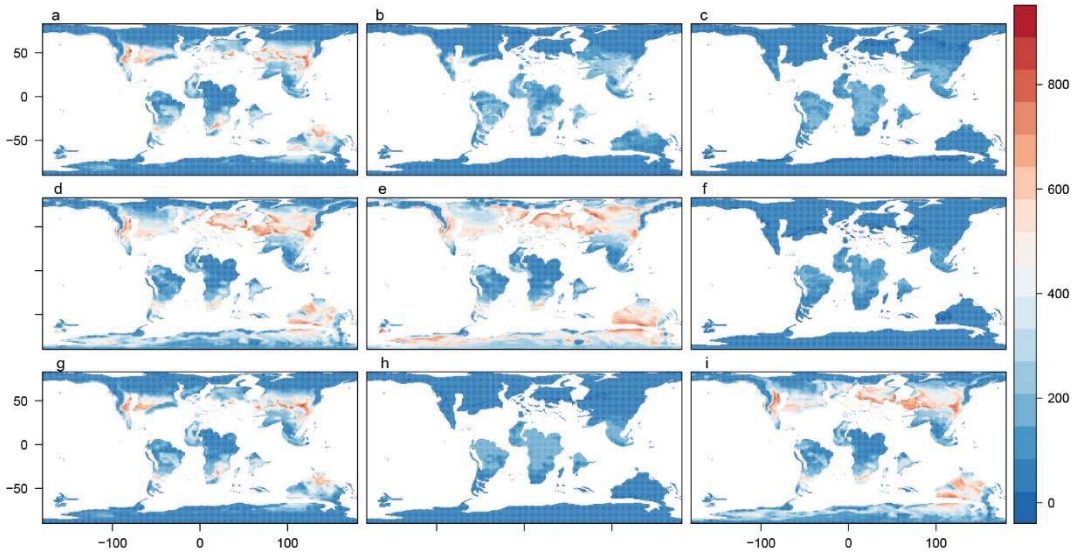

Figure 3. Ensemble habitat suitability models (averaged) projected globally for 9 clades of non-avian dinosaurs (additional details and figures on habitat suitability models are in Supplementary material). Blue color represents low level of habitat suitability (0), while red color represents high habitability (1000). Habitat suitability models trained on the Late Maastrichtian record and GCMs control (a), are then projected to decoupled solar dimming scenarios with 5% (Sc 1) of solar reduction (b) and (Sc 2) 10% of solar reduction (c). A climatic scenario modelling two different levels of greenhouse-enrichment due to the Deccan volcanism is reported in d (Sc 5) and e (Sc 6). The effect on the dinosaur suitable habitats for two transien simulations with Deccan volcanism inactive (F, Sc 11 and G, Sc 12) and active (H, Sc 13 and I, Sc 14), shows the dynamic response of global dinosaur habitability during the impact (F, Sc 11 and H, Sc 13) and throughout the recovery (G, Sc 12 and I, Sc14).

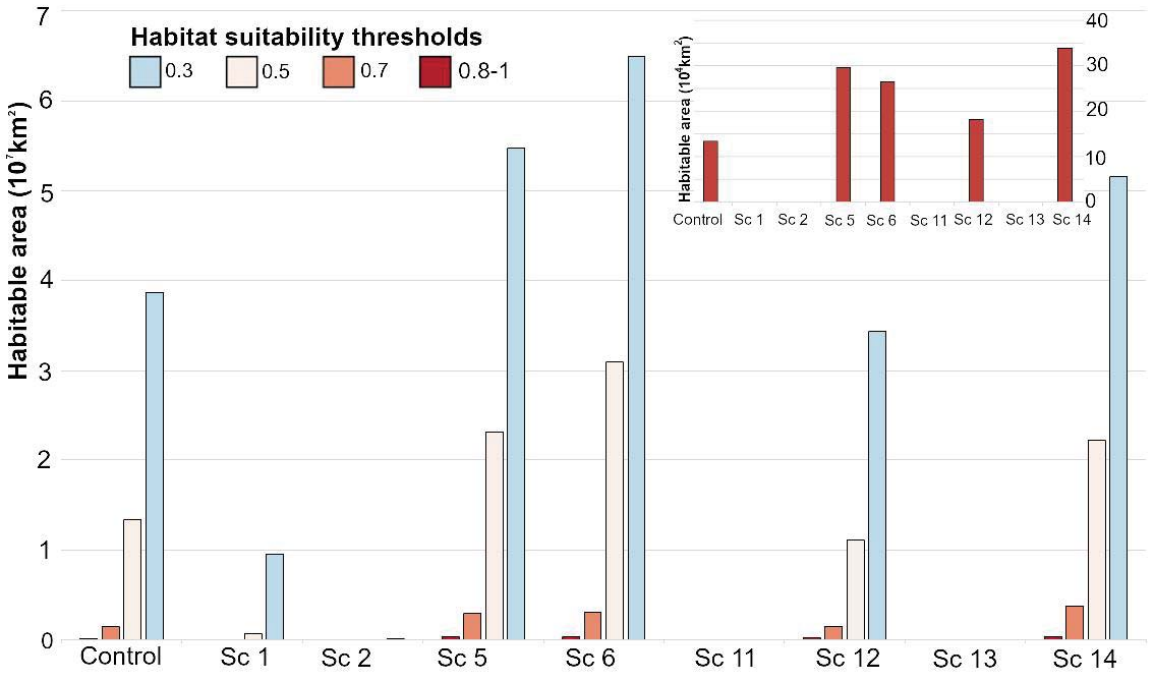

Figure 4. Histogram showing areal amount of habitat suitability for different ensemble HSM averaged in each climatic forcing scenarios (Sc) for all the clades used. A constant decrease from initial conditions (Control) is observed in the solar dimming models (Sc 1, 5% and Sc 2, 10%). A habitability increase is caused by a $\times 4CO_2$ (Sc 5) and $\times 6CO_2$ (Sc 6) addition. A transient model shows the habitability decrease during the impact-related climatic perturbation and consequent recovery, without Deccan volcanism (Sc 11 and Sc 12), and with active volcanism (Sc 13 and Sc 14).

775 **Table 1.** List of the K/Pg climate forcing scenarios used in this study. For the complete list check
776 Table S1. For a full description of all forcings please refer to Supplementary material.

Name in legends and text	Short description name	Description of simulation
Control	Maa_Cntrl	Late Maastrichtian Climate. Solar luminosity: 1357.18 W/m^2.
		Decoupled experiments
Scenario 1	Maa_-5%	5% solar dimming (modelling extreme Deccan cooling scenario or very mild Asteroid Impact scenarios). Solar luminosity: 1298.32 W/m^2
Scenario 2	Maa_-10%	10% solar dimming (Modelling lower extreme of impact-caused cooling). Solar luminosity: 1221.46 W/m^2.
Scenario 3	Maa_-15%	15% (Modelling moderate extreme of impact-caused cooling). Solar luminosity: 1153.6 W/m^2.
Scenario 4	Maa_-20%	20% (Modelling extreme of impact-caused cooling). Solar luminosity: 1085.74 W/m^2.
Scenario 5	Maa_4xCO_2	×4CO_2 (modelling 1120 ppm CO_2 injections caused by Deccan volcanism)
Scenario 6	Maa_6xCO_2	×6CO_2 (modelling 1680 ppm CO_2 injections caused by Deccan volcanism)
		Coupled experiments (transient)
Scenario 11	Aero100x_+Ash	Aerosol+Ash, During-Impact, ×100 Pinatubo
Scenario 12	Post_Aero100x_+Ash	Aerosol+Ash, Post-Impact, ×100 Pinatubo
Scenario 13	Aero100x_+4CO_2_+Ash	Aerosol+Ash+Deccan, During-Impact ×100 Pinatubo
Scenario 14	Post_Aero100x_+4CO_2_+Ash	Aerosol+Ash+Deccan, Post-Impact ×100 Pinatubo

777
778
779

780 **Table 2.** K/Pg climate forcing scenarios. The end-Cretaceous climate of the Maastrichtian
781 (control) and perturbations to the mean climate state resulting from a set of solar luminosity
782 (W/m2) reduction experiments at -5% and -10% (additional experiments are presented in
783 Supplementary material) and two different scenarios of CO2 injection due to Deccan volcanism.
784 Data are shown for Sea Surface Temperatures (SST; °C) at intermediate (666 m) ocean water
785 column depth; global, land and ocean Surface Air Temperatures (SAT; °C); and global, land and
786 ocean precipitation (mm/day) for the mean of the last 50-years of each simulation (see expanded
787 methods in Supplementary material).
788

	Ocean temperature		SAT			Precipitation		
Experiment	SST	666m depth	Ocean	Land	Global	Ocean	Land	Global
Control	22.64	12.41	21.65	11.49	18.96	3.5	2.38	3.2
-5% Sol. (Sc1)	16.93	12.06	14.87	1.83	11.42	3	2.05	2.75
-10% Sol. (Sc2)	11.06	11.72	4.56	-12.18	0.13	2.5	1.59	2.26
$2xCO_2$>$4xCO_2$ (Sc5)	25.11	12.56	24.47	16.2	22.28	3.58	2.49	3.29
$2xCO_2$>$6xCO_2$ (Sc6)	27.02	12.66	26.86	20.24	25.11	3.59	2.5	3.3

789
790

Table 3. Transient aerosol K/Pg extinction simulations. A set of transient simulations with perturbed aerosol atmospheric optical depth, pCO_2 concentrations and ash layer deposits is performed over a set of 200-year simulations. Their individual global, land and oceanic impact on specific climate variables (SST [°C], SAT [°C], Precipitation [mm/day]) for the 50-year mean pre-impact climate state and the mean of the 3 coolest years resulting from the post-asteroid impact. The complete set of experiments with sensitivity tests is presented in Supplementary material.

	SST		666 m depth:		SAT						Precipitation					
					Ocean		Land		Global		Ocean		Land		Global	
Experiment	Before Impact	Impact	Before Impact	Impact	Before Impact	Impact	Before Impact	Impact	Before Impact	Impact	Before Impact	Impact	Before Impact	Impact	Before Impact	Impact
Aerosol 100 with Ash deposit (Sc11-12)	22.1	2.49	11.81	11.88	21.38	-13.44	10.99	-30.21	18.63	-17.87	3.52	0.78	2.4	0.28	3.22	0.65
Aerosol 100 and 2xCO_2 >4xCO_2 with Ash deposit (Sc13-14)	23.93	4.05	11.81	11.88	23.59	-8.23	14.95	-25.96	21.31	-12.92	3.59	0.91	2.51	0.33	3.31	0.75

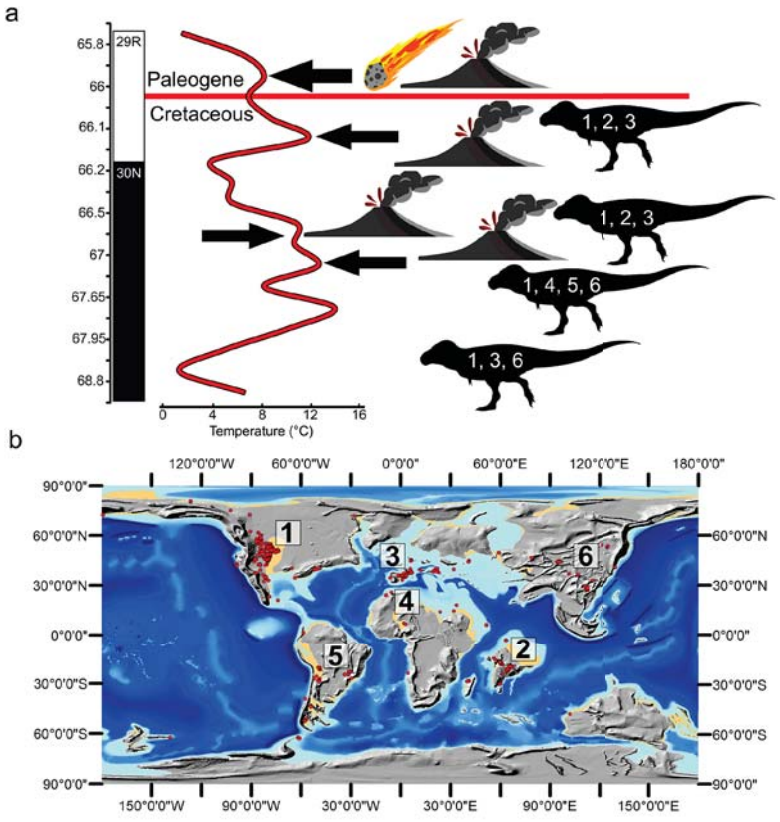
a
65.8
66
66.1
66.2
66.5
67
67.65
67.95
68.8
29R
30N
Paleogene
Cretaceous
1, 2, 3
1, 2, 3
1, 4, 5, 6
1, 3, 6
0
4
8
12
16
Temperature (°C)
b
120°0'0"W
60°0'0"W
0°0'0"
60°0'0"E
120°0'0"E
180°0'0"
90°0'0"
60°0'0"N
30°0'0"N
0°0'0"
30°0'0"S
60°0'0"S
90°0'0"
150°0'0"W
90°0'0"W
30°0'0"W
30°0'0"E
90°0'0"E
150°0'0"E
1
2
3
4
5
6

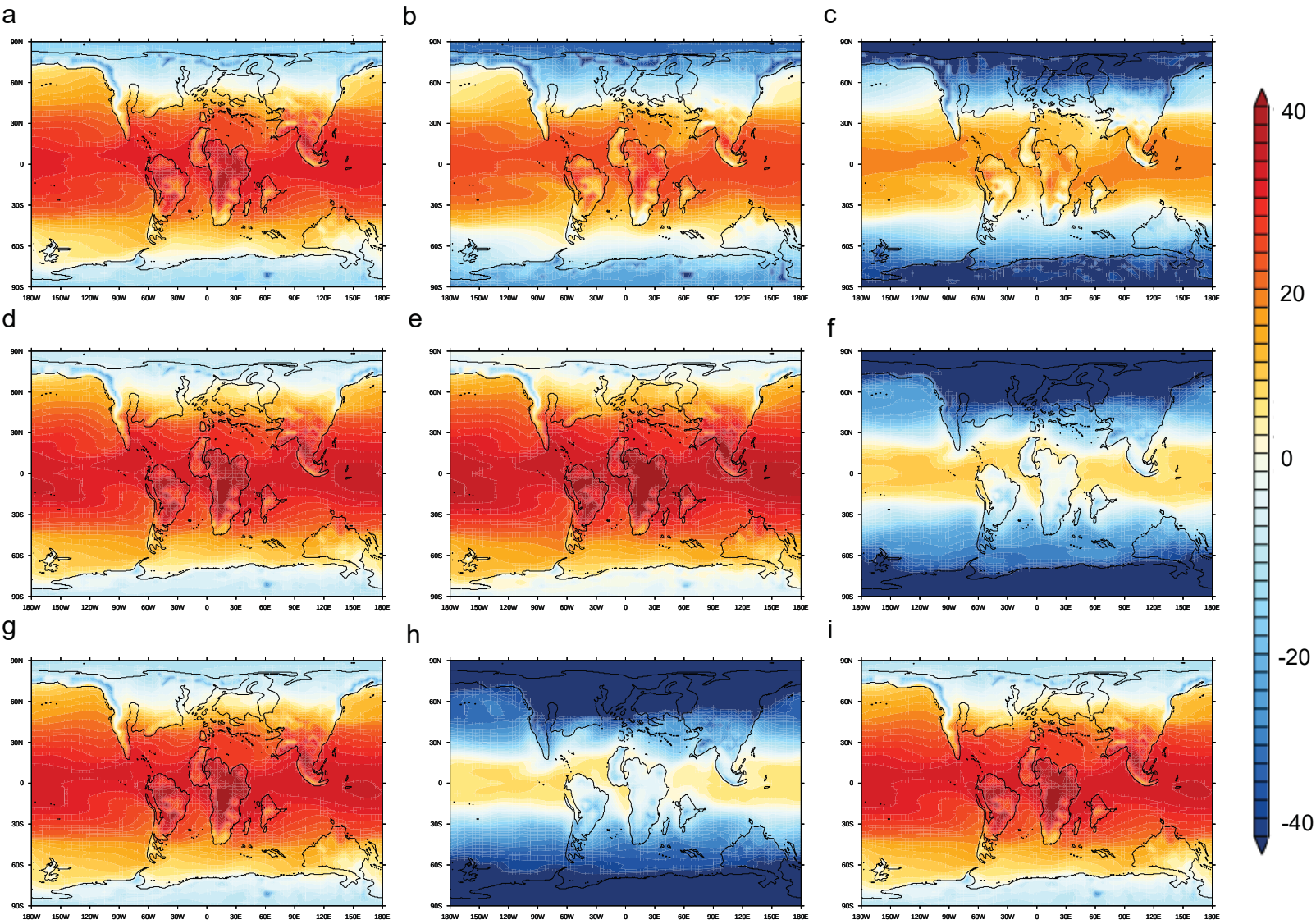
a
b
c
d
e
f
g
h
i
90N
60N
30N
0
30S
60S
90S
180W 150W 120W 90W 60W 30W 0 30E 60E 90E 120E 150E 180E
40
20
0
-20
-40

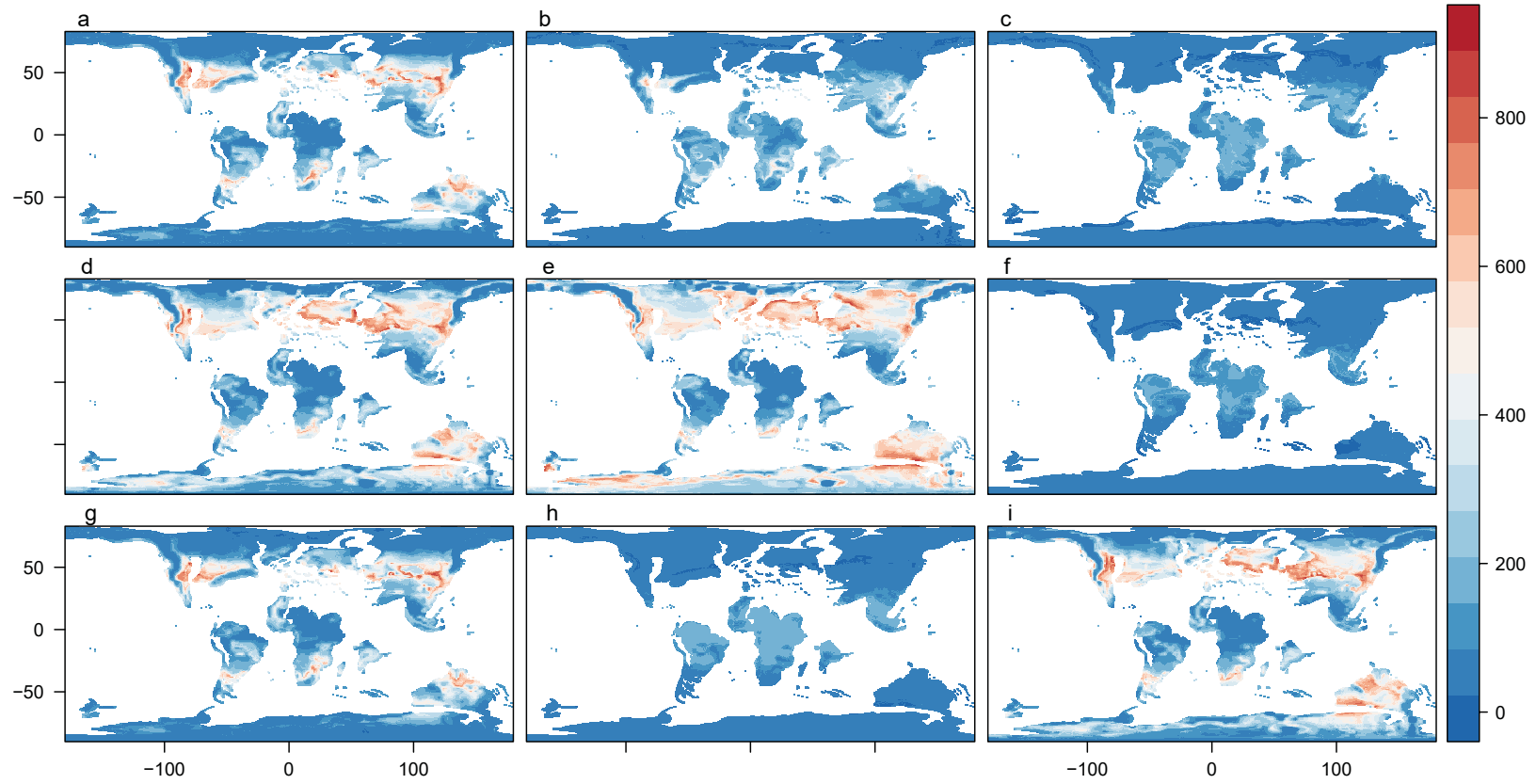
a
b
c
d
e
f
g
h
i
50
0
−50
−100
0
100
800
600
400
200
0

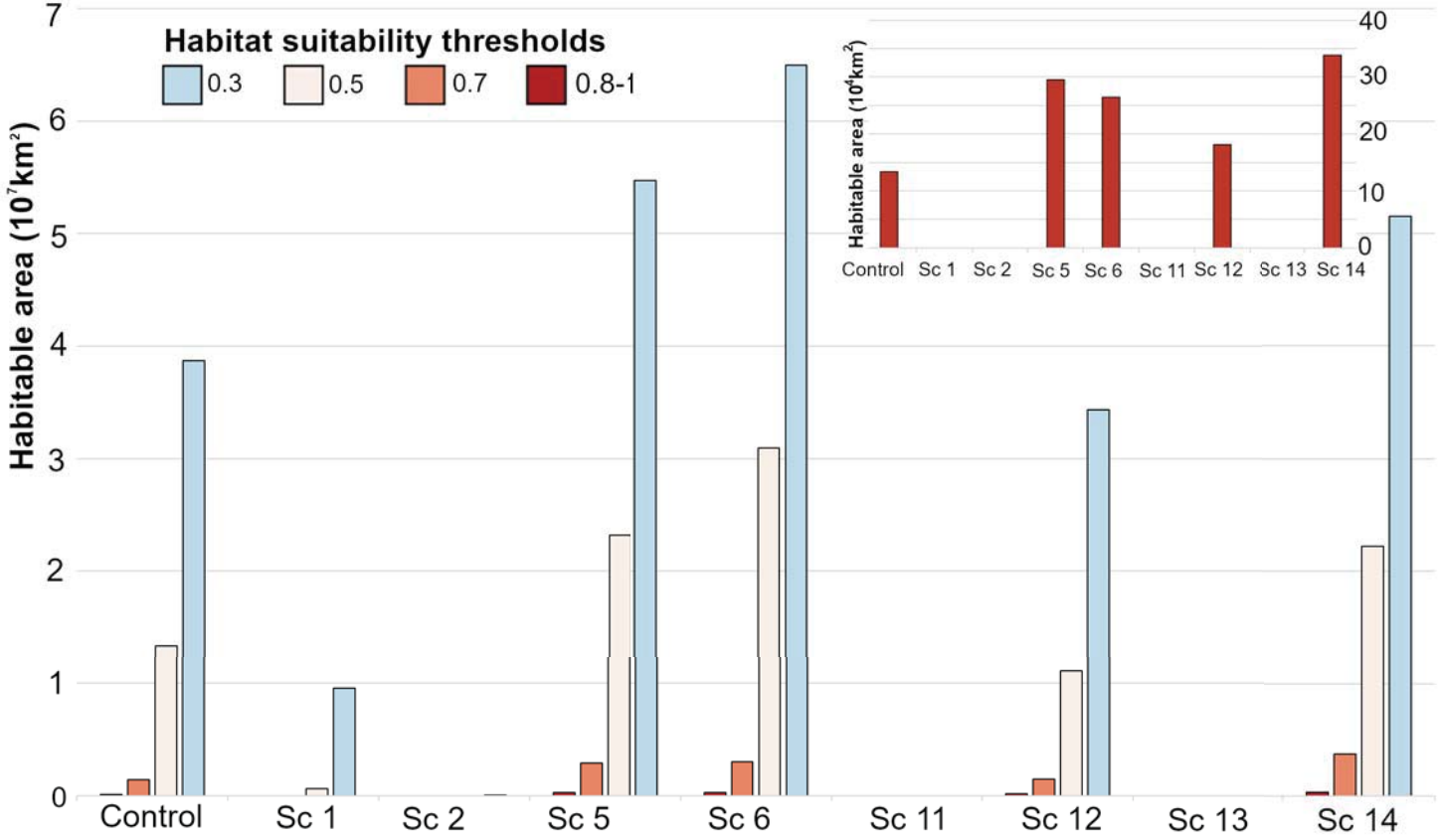
Habitat suitability thresholds
0.3
0.5
0.7
0.8-1
Habitable area (10^7 km^2)
0
1
2
3
4
5
6
7
Control
Sc 1
Sc 2
Sc 5
Sc 6
Sc 11
Sc 12
Sc 13
Sc 14
Habitable area (10^4 km^2)
0
10
20
30
40
Control
Sc 1
Sc 2
Sc 5
Sc 6
Sc 11
Sc 12
Sc 13
Sc 14

PNAS
www.pnas.org

Main Manuscript for

Asteroid impact, not volcanism, caused the end-Cretaceous dinosaur extinction.

Alfio Alessandro Chiarenza[1,2*†], Alex Farnsworth[3†], Philip D. Mannion[4], Dan J. Lunt[3], Paul Valdes[3], Joanna V. Morgan[1], Peter A. Allison[1].

1 Department of Earth Science and Engineering, Imperial College London, South Kensington, London, SW7 2AZ, UK.

2 Perot Museum of Nature and Science, Dallas, Texas, 75201, USA.

3 School of Geographical Sciences, University of Bristol, Bristol, BS8 1TH, UK.

4 Department of Earth Sciences, University College London, London, Gower Street, WC1E 6BT, UK.

†These authors contributed equally to this manuscript.

*Alfio Alessandro Chiarenza.

Email: a.chiarenza15@gmail.com

ORCID ID: https://orcid.org/0000-0001-5525-6730

Classification

Classification: Biological Sciences: Evolution

Keywords

Dinosauria, Extinction, End-Cretaceous, Chicxulub, Deccan

Author Contributions

A.A.C., A.F., P.D.M., P.A.A and J.V.M. conceived and designed the research; A.A.C., A.F., D.J.L. and P. V. produced and collected data; A.A.C. and A.F. analyzed the data; A.A.C. and A.F. produced the figures; A.A.C., A. F., P.D.M., and P.A.A. wrote the manuscript. A.A.C. and A.F. contributed equally to this work. All authors provided critical comments on the manuscript

This PDF file includes:

Main Text
Figures 1 to 4
Tables 1 to 3

Abstract

The Cretaceous/Paleogene mass extinction, 66 Ma, included the demise of non-avian dinosaurs. Intense debate has focused on the relative roles of Deccan volcanism and the Chicxulub asteroid impact as kill mechanisms for this event. Here we combine fossil-occurrence data with paleoclimate and habitat-suitability models, to evaluate dinosaur habitability in the wake of various asteroid-impact and Deccan volcanism scenarios. Asteroid-impact models generate a prolonged cold winter that suppress potential global dinosaur habitats. Conversely, long-term forcing from Deccan volcanism (CO_2-induced warming) leads to increased habitat suitability. Short-term (aerosol cooling) volcanism still allows equatorial habitability. These results support the asteroid impact as the main driver of the non-avian dinosaur extinction. In contrast, induced warming from volcanism mitigated the most extreme effects of asteroid impact, potentially reducing the extinction severity.

Significance Statement

This is the first quantitative test to our knowledge of end-Cretaceous extinction scenarios and how those would have affected dinosaur habitats. Combining climate and ecological modelling tools we were able to demonstrate a substantial detrimental effect on dinosaur habitats caused by an impact winter scenario triggered by the Chicxulub asteroid. We were not able to obtain such an extinction state with several modelling outputs from Deccan volcanism. We further show that the concomitant prolonged eruption of the Deccan traps might have acted as an ameliorating agent buffering the negative effects on climate and global ecosystems that the asteroid impact produced at the Cretaceous–Paleogene boundary.

Main Text

Introduction

The end-Cretaceous mass extinction, 66 million years ago (Ma), is the most recent of Raup and Sepkoski's (1982) 'Big Five' extinction events *(1, 2)*. Non-avian dinosaurs, along with many other groups that had dominated the Earth for 150 million years, went extinct. Although there is still debate as to whether dinosaurs were already in decline *(3)* prior to their extinction, their fossil record demonstrates global survival until the terminal Cretaceous and unambiguous absence afterwards. The Cretaceous/Paleogene (K/Pg) mass extinction coincided with two major global environmental perturbations: heightened volcanism associated with the Deccan Traps, and the Chicxulub asteroid impact (Fig. 1a) *(4)*. The relative roles of these two potential kill mechanisms on the timing and magnitude of the extinction have been fiercely debated for decades *(4, 5)*. The Maastrichtian has been shown to have a relatively high climate sensitivity *(6)* meaning even relatively small perturbations to the system could potentially have a catastrophic impact.

The Deccan Traps, in present-day west-central India *(7)*, formed from a series of short (~100 kyr) intermittent eruption pulses *(8)*, with two main phases *(8, 9)* at ~67.4 Ma (towards the end of the Cretaceous) and ~66.1 Ma (starting just before the boundary and continuing through the earliest Paleogene) erupting an estimated >10^6 km^3 of magma over the duration ~710,000 years *(9, 10)*. This volcanism released radiatively active atmospheric gases, particularly carbon dioxide (CO_2) and sulfur dioxide (SO_2), which are thought to have promoted global climate change *(11, 12)*. Most authors have argued for global average temperature excursions of ±2°C in relation to these pulses *(7, 8)* (though see ref *(9)* for a contrasting view on such correlations). Under this scenario, this potential kill mechanism either led directly to mass extinction *(5)*, or sufficiently stressed global ecosystems that they become vulnerable to subsequent agents *(13)*. Given that intense and prolonged volcanism appears to be the primary kill mechanism for earlier mass extinctions *(14, 15, 16)*, it is considered by some as the most likely candidate to explain the K/Pg mass extinction *(17)*. However, the timing and size of each eruptive event is highly contentious in relation to the mass extinction event *(8–10)*.

An asteroid, approximately 10 km in diameter, impacted at Chicxulub, in the present-day Gulf of Mexico, 66 Ma (*4, 18, 19)*, leaving a crater ~180–200 km in diameter (Fig. 1a). This impactor struck carbonate and sulfate-rich sediments, leading to the ejection and global dispersal of large quantities of dust, ash, sulfur, and other aerosols into the atmosphere *(4, 18, 19, 20)*. These atmospheric contaminants led to prolonged sunlight screening and global cooling (*19–22),* with severe ecological cascade effects *(4, 13, 23)*. The impact is hypothesized to have precipitated an extremely cold 'impact winter' that was beyond the thermophysiological limits of much of the end-Cretaceous biota *(23)*. A globally ubiquitous ejecta layer *(23)* overlies the latest Cretaceous fossiliferous horizons, marking a biotic change after the K/Pg boundary (Fig. 1a). The size of this impact, its hypothesized global climatic effects, and the worldwide absence of non-avian dinosaurs after it (Fig. 1b), suggest a direct causal relationship between these phenomena *(4, 23)*.

Several modelling approaches have attempted to reproduce the climatic conditions at the K/Pg boundary (*20–22)*, but none has so far quantified the abiotic effect on biological habitability. Herein, we model the climatic conditions at the end-Cretaceous, including the perturbations caused by the two potential extinction drivers. For the first time to our knowledge, we use Habitat suitability modelling to test the effect of these perturbations on the distribution of the dominant Cretaceous terrestrial group, the non-avian dinosaurs.

Results

The climatic perturbations generated by Deccan volcanism (67.4 Ma to 65.5 Ma *(24)*) and the asteroid impact (66.0 Ma *(25)*) are evaluated using coupled Atmosphere-Ocean General Circulation Model (AOGCM; forced by K/Pg boundary conditions) simulations (Fig. 2), which account for the combined effects of aerosol injection (ash, sulphate aerosol and soot deposition affecting surface light reflectance) that cool the climate, with secondary effects such as changes in surface albedo (snow and sea-ice feedback), as well as atmospheric gasses (CO_2) that warm the climate. Ozone concentrations are prescribed at modern-day values. The climate response is calculated using the mean of the last 50 years as well as the 3 years for the peak cooling event in the transient simulations. Climate simulations considered the effect of volcanism, both short-term aerosol injection (tens of years) and long-term CO_2 forcing (hundreds of years) and asteroid impact in isolation (decoupled, excluding long-term concurrent Deccan CO_2 forcing, experiments; Fig. S1–2), and together (coupled, inclusive of Deccan CO_2 forcing, experiments; Fig. S3–6), by means of transient aerosol forcing, where all climatic perturbations evolved with time (Fig. S7). Sensitivity experiments that varied the magnitude of the different perturbations were used to account for variations in the severity of these extreme events (Table S1; Supplementary material).

In the decoupled experiments (Table 1; Table S1), a 5% to 15% solar dimming reduction is considered to simulate the effects of Deccan volcanism or asteroid-induced cooling through reduction in incident SW (shortwave) radiation (-67.9 to -203.6 W/m^2), within the predicted range

of Kaiho et, al. *(18)*. However, the higher end estimate is considered too extreme by some regarding to Deccan, with Schmidt et al. *(16)* suggesting that the reduction in global mean surface temperature from a Deccan magnitude eruption represents no more than a -4.5°C reduction in surface cooling. This is less than the predicted cooling from in the 5% scenario (-9.7°C) suggesting atmospheric cooling as a result of Deccan volcanism will not drive swings in temperature and precipitation that would lead to an extinction level event.

These scenarios only represent a reduction in solar luminosity (in the case of -5% volcanism-induced solar dimming this assumes the best-case scenario [smallest climate forcing] whereby constant volcanic eruption allows replenishment of stratospheric aerosols at the same rate as aerosol loss from the stratosphere) without CO_2 release during 10^2 years of run time. As such, these solar dimming experiments give Deccan volcanism the best possible chance of inflicting an abiotic extinction level event through assuming long-term (1000 years) cooling (decreased solar forcing, mimicking constant aerosol loading of the stratosphere) that is yet to be proven in the rock record *(16)*. Further simulations, with solar luminosity reduced by 10%, 15% and 20% of the end-Cretaceous 'norm', evaluated progressively more extreme asteroid impact scenarios, which have been previously considered to be equivalent *(18, 25)* to a 10–20% lowering of solar input. Two additional simulations assessed the long-term (10^3 years) warming effect caused by Deccan volcanism resulting from increased atmospheric CO_2 release. Both represent extreme scenarios supported by long-term proxy evidence of an increase in atmospheric CO_2 from the 560 ppm baseline in the experiment to (i) 1120 ppm *(26)* and (ii) 1680 ppm *(27, 28)*.

The simulations show that solar dimming (Table 2; Table S2) would have generated global cooling of between 9.7°C to 66.8°C (in the most extreme scenario [20% solar dimming]; Fig. 2b, c; Table 2) on land, but that the addition of CO_2 from Deccan volcanism offset this cooling by warming of +4.7°C to +8.75°C (Fig. 2d, e; Table 2). Multi-proxy reconstructions from Hull, et al. *(10)* have shown a large pulse of Deccan CO_2 release prior to the K/Pg boundary led to only a 2°C warming *(10)*. More precise quantification is difficult because of the uncertain pace and magnitude of Deccan volcanism. Previous work *(26)* highlighted the short residence time of SO_2 in the stratosphere and suggested that the short transient nature (decadal duration) of the eruptions would not have enough long-term effect to force the climate into an extinction state. It has been argued *(16)* that even the 5% solar reduction scenario is an overestimate of the cooling effect of Deccan volcanism, and that a surface temperature cooling of 4.5°C is more likely (half that of the 9.7°C in our 5% solar diming scenario). The solar dimming scenarios would also affect the hydrological cycle. Modelled effects for 5% solar dimming include a 14% decrease and poleward shift in precipitation (Table 2; Fig. S1–3), whereas the most extreme (20%) asteroid-induced solar dimming scenario causes a 95% precipitation decrease.

Transient aerosol experiments (Table 1, 3), at the K/Pg event with and without ash deposition (scenarios 11–14), show a stark cooling (over the 6 year period where stratospheric aerosols are simulated) in global mean temperature (>34°C), followed by a recovery to 'normal', pre-boundary conditions (Fig. 2g–i; Table 3; Fig. S7) over a timeframe of decades. Here, two different transient aerosol-forcing experiments were conducted: (i) the K/Pg impact event based on inferred climate forcing as a result of aerosol release and land surface perturbation (*18, 20–22, 23–25*; Table 3) (with a sensitivity study in which this forcing was reduced by half; Table S3); and (ii) a set of simulations whereby release of CO_2 from Deccan volcanism was included (Table S3). These simulate aerosol loading from the asteroid impact (altering optical depth), as well as increased CO_2 from sustained long-term volcanism, both with simulated volcanogenic aerosol effect (Sc 9–14: Table 1; Fig. 2f, g), and without the latter volcanism-related effects (Sc 7, 8: Table 1; Fig. 2h, i). See Materials and Methods for further details (Supp. Info.). These simulations reproduce an impact that would have generated the same effect as 100 Pinatubo eruptions, hypothesized to be the same impact on climate as the Chicxulub impactor *(30)*. The Pinatubo eruption in 1991 led to the injection of 18–19 Tg of SO_2 into the lower stratosphere, with a 60-fold increase above non-volcanic levels. SO_2 concentrations were still 10x above normal after 2 years' equilibration time (e-folding) of 1 *(30)*. This led to planetary cooling of ~0.5 K and took 7 years for SO_2 to return to pre-eruption levels *(30, 31)*.

After the initial post-impact disturbance of the Cretaceous climate (peak land surface cooling to -34.7°C globally within 5 years; Fig. S7), our transient experiments (Table S3) indicate that the climate system recovery would have taken around 30 years; however, this would have been accelerated by ~10 years with the inclusion of volcanically-derived increased CO_2 (Fig. S7). In this case, the CO_2 would have enabled the climate to recover to 0±5°C within 10 years of the impact, and to pre-impact conditions after ~20 years. An ash layer over North America would have further offset ~4–5°C of land surface cooling, with a small enhancement in recovery to pre-impact temperatures (Fig. S7). The hydrological cycle over land would have been significantly modified, with precipitation reduced by over 85% (Table 3; Fig S1–3) in months after the impact.

Pre-impact end-Cretaceous climate data were used to identify the abiotic conditions favorable for non-avian dinosaurs (Fig. 3a; Methods). This was used as a baseline from which to evaluate the effect of the various modelled climate perturbations (incorporating the relative uncertainties to a suite of modelled climatic scenarios combined with Ensemble modelling *(32)* on the potential global distribution of non-avian dinosaur habitat (Fig. 3a). The 5% solar dimming experiment (Fig. 3b) leads to a disappearance in peak habitability from pre-K/Pg values, with potential habitat reduced to 4% and 24% in lower habitat suitability thresholds (0.5 and 0.3 respectively; Fig. 4). At 10% solar dimming, potential habitat is effectively removed, (0.4% of pre-K/Pg values; Fig. 3c) at the lowest habitability threshold (0.3; Fig. 4). Habitat suitability in solar dimming scenarios is completely extinguished at ≥15% dimming. Global habitability increases in models simulating long-term CO_2 injection due to Deccan volcanism, in case an asteroid impact would not have happened (Fig. 3d, e): maximum dinosaur habitat suitability increases by ~120% at 1120 ppm of CO_2 and ~97% at 1680 ppm of CO_2. These results suggest that long-term Deccan volcanism alone cannot be responsible for complete dinosaur habitat disruption, without invoking unrealistic volcanic SO_2 forcing (near-constant large ejections) not seen at any point in the Phanerozoic *(16)*. Habitat suitability modelling shows that regions of lower climatically suitable would still be present in more tropical latitudes for dinosaurs in the 5% and, to a lesser degree, in the 10% solar dimming scenarios (forcing too strong according to Schmidt et al. (*16*; Fig. 3). Habitat suitability reaches a critical threshold between the 10% and 15% solar dimming simulations, with no remaining habitat for non-avian dinosaurs in models with 15% dimming (Sc 3, Sc 4, Sc 7, Sc 8; Table 1). Chemical processes are not simulated in these experiments and could further lead to habitat loss.

The transient asteroid experiments show an extinction level event of the non-avian dinosaurs' climatic niche (Fig. 3f, h), coincident with the lowest temperatures reached in experimental simulations after asteroid-induced cooling (Fig. S3c, d). Habitat suitability for these taxa (Table S4) then re-establishes differentially in the models with and without long-term Deccan volcanism CO_2 increase. In scenarios simulating active volcanism (CO_2 increase), at the same time as the impact, maximum habitability increases of 152% from pre-impact levels after recovery (Fig. 3e, G; Fig. 4). In the transient experiments with inactive (no CO_2 release) Deccan volcanism, habitat suitability reaches lower levels than the pre-impact scenario, with 135% more of end-Cretaceous peak habitability once the ecosystem recovers from the impact (~30 years after). It is likely that in both scenarios this would return to pre-impact levels once the climate has fully re-equilibrated. In all transient asteroid impact model experiments for habitat suitability modelling (Table 3), the addition of Deccan-sourced CO_2 (Sc 13–14: Table 1) shows that the short-term transient cooling response is not significantly offset, and that eradication of non-avian dinosaur abiotic niche is pronounced (Fig. 3, 4). On the other hand, recovery rates are accelerated, and post-extinction habitability is re-established at a relatively higher level when coincident volcanism is modelled during the post-impact scenario.

An independent run using MaxEnt *(33, 34)* was performed to test whether these results would corroborate the outcome from the Ensemble simulations (see Methods and Supplementary Material). The 5% solar dimming experiment leads to a substantial, but non-catastrophic, 50% reduction in peak habitability from pre-K/Pg values (Fig. S18a, b). With 10% solar dimming, potential habitat is reduced to 4% of pre-K/Pg values (Fig. S18c), and extinguished at ≥15% dimming. Global habitability is higher in models simulating constant CO_2 injection due to Deccan

volcanism (Fig. S18d, e): maximum dinosaur habitat suitability increases by ~27% at 1120 ppm of CO_2 and ~32% at 1680 ppm of CO_2, confirming the previous Ensemble results in which long-term Deccan volcanism alone cannot be found responsible for complete dinosaur climatic niche extirpation. The simulated transient asteroid impact experiments (Fig. 18f–h) confirm the same trends of the Ensemble outputs (Fig. 3f, h), in providing an almost complete eradication of dinosaur abiotic niche. Even here habitat suitability for these taxa (Table S4) re-establishes more quickly and at higher 'pre-extinction level' when active Deccan volcanism-induced CO_2 injection is simulated as active (122% of pre-impact levels after recovery [Fig. 18e, g; Fig. 19]). Analogously with the Ensemble results, inactive Deccan volcanism fosters a recovery to 92% of end-Cretaceous, pre-impact habitability.

Discussion

The view of Deccan volcanism (both short and/or long term) as the main abiotic driver of the K/Pg mass extinction is often justified by referring to volcanism as a historically strong influencer of global climate *(11, 12)*. Most pertinently, extensive volcanism is recognized as the primary cause behind the most severe biotic crisis of all time, the end-Permian mass extinction, 251 Ma *(35)*, and possibly the Triassic/Jurassic mass extinction, 201 Ma (*15*). However, the timing and duration of the end-Permian extinction was quite different from that of the K/Pg event, with some organisms disappearing earlier than others *(36)* over the course of ~10 myr. The ocean also acidified and became anoxic, which is symptomatic of a geologically slow process *(37–39)*. All of this indicates a prolonged and multiphase extinction process *(35)*. Furthermore, a recent study found no correlation between the timing of Deccan volcanism pulses and global climate changes *(9, 10)* or a large pulse 10^4 prior to the bollide impact questioning Deccan volcanism's influence as an abiotic driver of extinction *(8)*. It is noteworthy that even the stratigraphic inter-beds of the Deccan Traps have yielded dinosaur and other terrestrial fossil remains *(40, 41;* Fig. 1*)*, indicating that animals were able to survive previous high intensity eruptions, even within the epicenter of the Deccan region itself. Given India's geographic isolation at this time, these fossil-bearing beds cannot be explained by biotic restocking via dispersal events *(40)*. Short-term Deccan volcanism (aerosol release), even in the more extreme Deccan-induced 5% solar reduction scenario (with greater sulfur release than hypothesized *(16)* does not perturb the mean climate state sufficiently to produce an inhospitable biosphere globally for non-avian dinosaurs. Even assuming the highest intensity of sulfur injections caused by Deccan volcanism (and longest atmospheric residence times), the order of magnitude of these releases barely approaches the lowest estimates of release by the Chicxulub impactor *(20–22)*. Longrich *(42)* proposed that mammal diversity in latest Cretaceous assemblages (e.g. the North American Hell Creek Formation *(43–45)* actually increases following the Deccan eruption. Given that the hypothisised *(25)* asteroid induced-cooling likely drove the extinction, a pulse of warming (with a similar magnitude as shown in our simulations) *(9)* just prior to the extinction may have actually played as a buffer against cooling induced by the Chicxulub impact, ameliorating the physical effects of bolide impact *(42)*. Such scenario seem to be supported by the recently described continental record of biotic recovery across the K/Pg boundary *(43)*, in which Lyson et al. *(43)* presented stratigraphic and palaeontological evidence of mammalian increase in diversity and body size, coinciding with warming pulses and radiation of major angiosperm clades, and suggesting a possible link with Deccan-induced greenhouse gasses enriching effect.

Even within the site of the asteroid impact, rich communities were re-established within 30 kyr of the K/Pg boundary *(46)*. This implies a very rapid recovery of marine productivity *(46, 47)*, which argues against the suggested delay in ecosystem reset caused by continued Deccan volcanism after the K/Pg boundary *(9, 46, 47)*. In contrast to the end-Permian mass extinction, the K/Pg event was geologically instantaneous *(2–4, 10, 23, 36)*, and there is no clear evidence for a prolonged decline *(3, 4, 36, 48*) that would be required for Deccan volcanism to trigger a mass extinction level event due to the short residence time of stratospheric aerosols. In addition, studies on marine macrofossils from Antarctica are consistent with a sudden, catastrophic driver for the extinction, such as the bolide impact, rather than a significant contribution from Deccan

Traps volcanism during the latest Cretaceous *(49)*. Although some authors have argued for a latest Cretaceous decline in dinosaur diversity, other analytical studies are consistent with relatively high pre-extinction standing diversity, which is compatible with a sudden extinction scenario for non-avian dinosaurs *(48)*. The extinction of only shallow-water marine organisms *(12, 46, 49–51)* highlights a lack of prolonged deep-water acidification, while conjoined isotopic and Earth System Modelling results show rapid oceanic acidification *(50)* and subsequent quick recovery *(50)* compatible with asteroid induced effects in the ocean. One major implication of such a quick event for the marine realm is that the extinction driver must have been in play for a duration shorter than the mixing time of ocean waters (~one thousand years) *(46, 50)*. Our simulations (Tab. 1–2) suggest that sea surface temperatures would have been reduced for all scenarios (Fig. S1, S3, S5, S7), but that the rest of the water-column (>1000 m) was unaffected (Fig. S7b). After the extinction, the marine environment recovered relatively fast, between a few thousand to ~one million years *(9, 46, 47, 50)*.

Whether or not Deccan volcanism actively contributed to temperature decline through atmospheric cooling (via SO_2 aerosol release) is still unclear. The emissions resulting from Deccan volcanism also caused a local atmospheric injection of gas and debris *(24, 28)*, reflecting incident solar radiation from the Sun, but potentially trapping radiant heat in the lower level of the atmosphere *(8, 11, 14)*. It is unclear whether the volatile products from the Deccan reached the stratosphere. With SO_2 stratosphere-residence times being of the order of years, pacing of eruptions would have had to be significant, with sustained high energy activity over 10–100s of years *(16)* to inject a constant supply of climate-cooling aerosols to achieve extinction-driving levels. This rate of volcanism would also have to be at an intensity that would represent a 15–20% reduction in solar luminosity range whose climatic impact is shown to be far beyond that hypothesized *(16)*. Long-term Deccan CO_2 warming would have led to an expansion of dinosaur habitable regions in this study, although the global warming we simulate is slightly higher than suggested by proxy-records (~3°C in scenario 5 as opposed to ~2°C *(10)*. A longer-term effect of volcanism would directly (and potentially indirectly through a weakened alkalinity pump *(50)*) increase CO_2 content offsetting individual short-term cooling events and increasing habitability.

We show that the abiotic impact of Deccan volcanism was not sufficient to cause the extinction of non-avian dinosaurs, while the effects of the impact alone were enough to cause the extinction. It is more likely that the Deccan's influence after the event might have been of greater importance in determining ecological recovery rates after the asteroid-induced cooling, rather than delaying it *(43)*. This also fits well with a recent recalibration that suggests that much of the heightened volcanic activity occurred after the K/Pg boundary *(9, 10)*.

The lithology of the target rocks collided by the Chicxulub asteroid led to a massive release of hundreds of Gt of sulfates *(21, 22, 29)*, yet it is unknown how much reached the stratosphere *(16)*, with a correlated cooling effect of 27° C (22). This would have led to 3 to 16 years of sub-freezing temperatures and a recovery time of more than 30 years. Results from the most recent IODP drilling expedition *(29)* suggest that the estimate of sulfur injected to the atmosphere by the impact should be much higher (325 ± 130 Gt of sulfur and 425 ± 160 Gt of CO_2), which might have generated cooling for centuries *(37)*. Clearly, the asteroid impact was devastating to Earth's climate, leading to freezing temperatures on land (simulated duration in herein reported experiments of ~30 years), even at the tropics, disrupting large faunal food supply and destabilising all trophic levels.

Non-avian dinosaurs were not the only victims of the K/Pg mass extinction. Other vertebrate taxa, such as birds *(52, 53)*, mammals *(54, 42)*, and squamates *(55, 56)*, were affected by severe extinction rates *(57)*, whereas other groups, such as crocodylomorphs, turtles, and choristoderes were affected to a lesser degree *(57–60)*. Without even accounting for other terrestrial and marine animals affected (or completely wiped out, *(1, 61, 62)*, it appears that organisms from a vast array of different ecologies were hit by the extinction mechanism. An ecological determinant behind the high selectivity of the process may be found in variables like body size, diet, physiology, habitat, and geographic range *(5, 57, 63)*. Many of these ecological traits can be, to a certain degree, linked to temperature fluctuations. We know for example that habitat, body size, and geographic ranges in living members of crown group Archosauria are extremely sensitive to

thermal excursions *(63–65)*. Ecosystem structure can also be severely affected by drastic temperature variations, with an important impact on biodiversity *(66, 67),* as it has already been suggested for the K/Pg mass extinction *(13)*. An ecological refugium-role, potentially offered by the higher thermal inertia of freshwater environments, microhabitats, or the trophic opportunities provided by the detritus cycle *(57, 68)*, may be a potential explanation behind this differential survivorship process. Refugia from extinction level temperature excursion might have been found in deep valleys, fluvio-lacustrine systems, coastal regions, and in the tropics, which would have offered shelter for taxa such as birds, mammals, turtles, crocodiles, lizards, and snakes, all of which survived the K-Pg mass extinction with comparatively little species loss *(42, 43, 45, 53, 55)*. Lowered biotic barriers *(69)* coinciding with warming pulses (*9*) that sped-up the thermic recovery of Earth System, might have boosted an ecological recovery and consequent release across the boundary in the earliest Danian *(10, 42, 43)*.

These elements imply a cause-effect relationship between the Chicxulub impactor and the K/Pg mass extinction of non-avian dinosaurs. Furthermore, GCMs and habitat suitability modelling simulations suggest that climatically active volcanic by-products might have sped up recovery after an impact winter-induced mass extinction. If this is the case, the perception of Deccan volcanism as a K/Pg extinction driver might need to shift to a new paradigm which emphasizes the mitigating effect that volcanism could have had on global cooling. Our results support the Alvarez hypothesis *(23)*, which attributes the end-Cretaceous mass extinction to a prolonged impact winter, as the most likely explanation for the extinction of non-avian dinosaurs. Although we do not discount the impact from biotic effects or other, not tested here, abiotic drivers (e.g. wildfire, acid rain), these results show that even without them the impact winter would have led to dinosaur demise. We demonstrate possible climatological threshold necessary to trigger the complete extinction of non-avian dinosaurs. Furthermore, we suggest that Deccan volcanism might have contributed to the survival of many species across the K/Pg boundary, and potentially fostered the rapid recovery of life from the most iconic of mass extinctions. This modeling approach has the potential to be used for clades (where sampling is spatially and temporally abundant and robust) to de-convolve the impact of secular climate change as a result of various abiotic forcings.

Although we focus on a more likely terrestrial asteroid impact *(18)* it has been suggested that a deep ocean impact that does not reach the bathymetric surface could result in a substantial injection of water vapour into the stratosphere. It has been suggested that in such a scenario that increased oceanic derived stratospheric water vapour may have cancelled out any aerosol cooling effect and led to significant surface warming *(70)*. Future studies should focus on investigating the effect of other abiotic drivers (e.g. acidification, halogens, significant surface warming, UV radiation, fire, carbon cycle disruption) of both asteroid impact and Deccan volcanism, as this may offer another avenue to understand the relative effect of both events.

Materials and Methods

General circulation models of end-Cretaceous extinction scenarios

The climate simulations were carried out using the coupled Atmosphere-Ocean General Circulation Model (AOGCM), HadCM3L-M2.1 *(71)*). HadCM3L has contributed to the Coupled Mode Intercomparison Project (CMIP) experiments demonstrating skill at reproducing the modern day climate *(71, 72)* and has been used for an array of different paleoclimate experiments *(73–75).* Unlike previous studies using AOGCMs *(18*, *76–78)* to explor the effect of end-Cretaceous volcanism and asteroid impact (and associated aerosol ejecta) we do not use a modern-day topography and bathymetry, but a geologic stage specific boundary conditions representative of the end-Cretaceous palaeogeography instead *(6)*. Carbon dioxide concentrations at the end-Cretaceous were set to 560 ppm, within the range of recent pCO_2 reconstructions *(79, 80)*.

The simulations of the extinction scenarios (Table S1) are separated into their (1a) short-term and (1b) long-term impact on climate and ultimately non-avian dinosaur abiotic niche. The simulation of Deccan volcanism scenarios is obtained by perturbing the climate by either: 2a -

sustained stratospheric sulfate aerosol loading, or 2b - sustained increased CO_2. Because of uncertainty in the amount of aerosol release from such events, we investigate the impact of volcanism as a function of a constant reduction in solar radiation (solar dimming) at the Earth's surface simulating the radiative cooling effect of sulphate aerosols in the stratosphere. A reduction in solar radiation equal to 5-15% has been hypothesized to be comparable for Deccan volcanism (without CO_2 release) *(24, 79–81)*. To test uncertainty of Deccan volcanism stratospheric aerosol loading and associated cooling we also test the impact of 15-20% solar reduction, which can also be used synonymously as an asteroid impact solar luminosity reduction analogue due to predicted change in radiative forcing *(25)*.

Sustained volcanic release of CO_2 has been hypothesized *(81– 84)* as a potential mechanism of extinction in the end Cretaceous. Two idealized large injections of CO_2 have been simulated over a 200-year period. Both represent extremes scenarios supported by geological evidence of an increase in CO_2 from the 560 ppm baseline CO_2 in the model to i) 1120 ppm *(26)* and ii) 1680 ppm *(16, 27)* CO_2. Previous attempts in constraining the total volume of eruptive material and volatiles *(26)* refer to a CO_2 release of ×2.1–4 times, so that our ×4CO_2 scenario models an extreme Deccan release. Numerical values for the physical parameters in the decoupled (Table S2), and transient coupled (Table S3) are reported.

We prescribe stratospheric sulphate aerosol concentrations as a function of the impact on atmospheric optical depth to simulate an extraterrestrial asteroid impact. Optical depths at 0.55μm were taken from observations *(27)* of the 1991 Pinatubo eruption with sulphate aerosol loading of the stratosphere equivalent to 100 times the forcing of the Pinatubo eruption *(27, 20)* consistent with the estimates of Pierazzo, et al. *(20).* The radiative impact of sulphate aerosols is simulated through absorbing and scattering incoming solar radiation across a spectral range of 0.2–10 μm assuming a constant aerosol size distribution *(85)*. A Stratospheric residence time of ~6 years for the sulphate aerosol was implemented taking into account the longer hypothesized residence time of Pierazzo *(20–22)* due to increased atmospheric stratification as a result of concurrent surface cooling and stratospheric warming *(86).* Stratospheric injection of aerosols into the model was initialized at year 40 into the 200-year simulation. Outside of this 6-year asteroid impact aerosol injection window, no aerosols were released as there is no known baseline aerosol concentration for the Maastrichtian time period to apply. To test the sensitivity of the 100× Pinatubo forcing, we also simulate the impact of a less severe asteroid impact with a 50× Pinatubo set of simulations. The individual impacts of increased CO_2, ash layer, and a 100× and 50× Pinatubo aerosol forcing were also simulated. Explanations for all simulations are listed in Table S1.

Episodic eruptions over the last 350 kyr of the Cretaceous would have increased the amount of CO_2 in the atmosphere and so we also consider a set of simulations with and without the impact of CO_2 degassing as a result of Deccan volcanism (Table S2). CO_2 will have the competing effect of increasing global temperature potentially offsetting the impact of cooling from stratospheric sulfate aerosols. The precise amount of CO_2 released from Deccan volcanism is unknown due to the difficulty in constraining the total volume of eruptive material and volatiles *(24)*. Here we use a conservative approach by doubling the baseline CO_2 concentration at the start of the simulation. This is greater than predicted for even the most extreme scenarios *(24, 87)*. Although the amount is likely unrealistic, this does evaluate the potential of volcanically derived CO_2 to mitigate for the cooling effects of impact-derived SO_2.

A set of simulations with and without a continental size ash blanket *(88)* over North America (latitudes 67.5°N to 15°N and longitudes 26.25°W to 116.25°W) that may have occurred from the fallout are also performed. For simplicity and due to the uncertainty in the longevity of the ash layer we prescribed the ash layer for the duration of the 200-year simulation. For the composition of the imposed ash layer and soil properties from observations we follow Jones, et al. *(88)*.

A reduction in solar radiation of -5%, -10%, -15% and -20% of Maastrichtian solar luminosity is reproduced for increasingly more extreme asteroid impact scenarios (a solar dimming between 10–20% has been discussed in published estimates for atmospheric radiative transfer models of sunlight filtration at the K/Pg event) *(24, 25)*. These are obtained by reducing solar luminosity by

5%, 10%, 15% and 20% for a 200-year period under 2xCO_2 conditions (Table S2). This allows a range of hypothesized impact events simulating the effect of different potential magnitudes. See supplementary material for expanded discussion and figures on baseline boundary conditions and simulation of the different extinction scenarios.

Dinosaur occurrence dataset

The fossil occurrence dataset was assembled by downloading a comprehensive database of late Maastrichtian (69–66 Ma) global dinosaur fossil occurrences from the Paleobiology Database (PaleobioDB: https://paleobiodb.org) on 6th April 2018 (Supplementary Data S1-2) which have been properly checked for accuracy and cleaned to obtain a dataset of 2088 entries. These occurrences belong to 9 clades of the end-Cretaceous global dinosaurian fauna *(76)* and comprise the: Ankylosauria, Ceratopsidae, Deinonychosauria, Hadrosauridae, Ornithomimosauria, Oviraptorosauria, Pachycephalosauridae, Sauropoda and Tyrannosauridae. Expanded discussion on spatial occurrences preparation is reported in the Supplementary Material.

Habitat suitability modelling

GCM-derived environmental variables were chosen based on broad autecological analogy with their most closely related living organisms ([crocodiles + birds *(89–91)*]). We used Pearson's pairwise correlation test to determine co-linearity between variables (Fig. S8), keeping only the predictors showing a Pearson's correlation coefficient below 0.7 to prevent overfitting. The climatic variables used for our habitat suitability modelling (HSM) were the temperatures of the warmest and coldest annual quartiles and the precipitation of the wettest and driest yearly quarters (Fig. S9–17). These analyses were run in R version 3.5.1 (R core team 2018) with the biomod2 package *(92, 93)* for Ensemble modelling *(32)* and using MaxEnt (maximum entropy algorithm *(33, 34)*) in the java platform version 3.4.1.

All raw data (environmental variables and occurrence data) and modelling outputs are reported in the Supplementary material of this article (Data S1–14).

Expanded discussion on HSM and figures on additional HSMs are presented in supplementary material, with all settings from Ensemble and MaxEnt modelling reported. The scripts for habitat suitability quantification in areal extent are reported in Data S13-S14.

Acknowledgments

We are grateful for the efforts of all those who have generated Maastrichtian dinosaur fossil data, as well as those who have entered these data into the Paleobiology Database, especially Matthew Carrano and John Alroy. We thank Getech, PLC. for providing palaeogeographic base maps, digital elevation models and palaeorotation of fossil occurrences used in this study. Lewis Jones (Imperial College London) is thanked for relevant discussions on habitat suitability modelling. Jack Mayer Wood is thanked for the dinosaur silhouette reported in Figure 1 and used under CC BY 3.0 license (https://creativecommons.org/licenses/by/3.0/ CC BY 3.0). Christopher Dean (University of Birmingham) is acknowledged for scientific discussion relevant to this study. A.A.C. was supported by an Imperial College London Janet Watson Departmental PhD Scholarship, A.F. and D.J.L. acknowledge NERC grant NE/K014757/1, Cretaceous-Paleocene-Eocene: Exploring Climate and Climate Sensitivity, P.D.M. was supported by a Royal Society University Research Fellowship (UF160216).

References

1. D. M. Raup, J. J., Jr. Sepkoski, Mass extinctions in the marine fossil record: *Science*, **215**, 1501-1503 (1982).
2. D. E. Fastovsky, P. M. Sheehan, The extinction of the dinosaurs in North America. *GSA Today* **15**, 4 (2005).
3. A. A. Chiarenza *et al*., Ecological niche modelling does not support climatically-driven dinosaur diversity decline before the Cretaceous/Paleogene mass extinction. *Nat. Commun*. **10**, 1091 (2019).
4. P. Schulte *et al*., The Chicxulub asteroid impact and mass extinction at the Cretaceous-Paleogene boundary. *Science* **327**, 1214–1218 (2010).
5. J. D. Archibald *et al*., Cretaceous extinctions: multiple causes. *Science* **328**, 973 (2010).
6. A. Farnsworth *et al*., Climate sensitivity on geological timescales controlled by nonlinear feedbacks and ocean circulation. *Geophy. Res. Lett.* **46**, 9880–9889 (2019).
7. V. E. Courtillot, P. R. Renne, Sur l'âge des trapps basaltiques (On the ages of flood basalt events). *Comptes Rendus Geosc.* **335**, 113–140 (2003).
8. B. Shoene *et al*., U-Pb constraints on pulsed eruption of the Deccan Traps across the end-Cretaceous mass extinction. *Science*, **363**, 862–866 (2019).
9. C. J. Sprain *et al*., The eruptive tempo of Deccan volcanism in relation to the Cretaceous-Paleogene boundary. *Science*, **363**, 866–870 (2019).
10. P. M. Hull *et al*., On impact and volcanism across the Cretaceous-Paleogene boundary. Science **367**(6475), 266-272, 10.1126/science.aay5055 (2020).
11. D. L. Royer *et al*., CO_2 as a primary driver of Phanerozoic climate. *GSA Today*. **14**, 4–10, 10.1130/1052-5173 (2004).
12. P. Wilf, K. R. Johnson, B. T. Huber, Correlated terrestrial and marine evidence for global climate changes before mass extinction at the Cretaceous-Paleogene boundary. *Proc. Natl. Acad. Sci. U.S.A.* **100**, 599, 10.1073/pnas.0234701100 (2003).
13. J. S Mitchell *et al.*, Late Cretaceous restructuring of terrestrial communities facilitated the end-Cretaceous mass extinction in North America. *Proc. Natl. Acad. Sci. U.S.A.* **109**, 18857–18861 (2012).
14. P. R. Renne *et al.,* Time scales of critical events around the Cretaceous-Paleogene boundary. *Science*, **339**, 684, 10.1126/science.1230492 (2013).
15. D. P.G. Bond, P. B. Wignall, Large igneous provinces and mass extinctions: An update", Volcanism, Impacts, and Mass Extinctions: Causes and Effects, Gerta Keller, Andrew C. Kerr. *GSA Special Papers*, **505,** 10.1130/SPE505 (2014).
16. A. Schmidt *et al*., Selective environmental stress from sulphur emitted by continental flood basalt eruptions. *Nat. Geosci.* **9**, 77-82 (2016).
17. E. Font *et al.,* Deccan volcanism induced high-stress environment during the Cretaceous–Paleogene transition at Zumaia, Spain: Evidence from magnetic, mineralogical and biostratigraphic records. Earth and Planetary Science Letters. **484**, 53-66, 10.1016/j.epsl.2017.11.055 (2018).
18. K. Kaiho *et al.*, Global climate change driven by soot at the K-Pg boundary as the cause of the mass extinction. *Sci. Rep.* **6**, (2016).
19. J. Vellekoop *et al.,* Rapid short-term cooling following the Chicxulub impact at the Cretaceous–Paleogene boundary. Proc. Natl. Acad. Sci. USA **111**, 7537-7541 (2014).
20. E. Pierazzo, A. N. Hahmann, L. C. Sloan, Chicxulub and climate: Radiative perturbations of impact-produced S-bearing gases. *Astrobiology* **3**, 99, 10.1089/153110703321632453 (2003).
21. J. Brugger, G. Feulner, S. Petri, Baby, it's cold outside: Climate model simulations of the effects of the asteroid impact at the end of the Cretaceous, Geophys. Res. Lett. **44**, 419–427 10.1002/2016GL072241 (2017).
22. K. O. Pope, K. H. Baines, A. C. Ocampo, B. A. Ivanov, Energy, volatile production, and climatic effects of the Chicxulub Cretaceous/Tertiary impact. J. Geophys. Res. 102, (E9), 21645, 10.1029/97JE01743 (1997).

23. L. W. Alvarez, W. Alvarez, F. Asaro, H. V. Michel, Extraterrestrial cause for the Cretaceous-Tertiary extinction. Science **208**, 1095, 10.1126/science.208.4448.1095 (1980).
24. A.-L. Chenet *et al.*, Determination of rapid Deccan eruptions across the Cretaceous-Tertiary boundary using paleomagnetic secular variation: 2. Constraints from analysis of eight new sections and synthesis for a 3500-m-thick composite section. *J. Geophys. Res.* **114**, (B6), B06103, 10.1029/2008JB005644X (2009).
25. K. Pope, K. Baines, K. Ocampo, B. A. Ivanov. Impact winter and the Cretaceous/Tertiary extinctions: Results of a Chicxulub asteroid impact model, *Earth and Planetary Science Letters* **128**, 719-725 (1994).
26. T. S. Tobin, C. M. Bitz, D. Archer, Modeling climatic effects of carbon dioxide emissions from Deccan Traps volcanic eruptions around the Cretaceous-Paleogene boundary. *Palaeogeogr. Palaeocl.* **478**, 139-148 (2017).
27. M. Sato, J. E. Hansen, M. P. Mccormick, J. B. Pollack, Stratospheric Aerosol Optical Depths, 1850-1990. J. Geophys. Res-Atmos. **98**, 22987-22994 (1993).
28. S. Self, M. Widdowson, T. Thordarson, A. E. Jay, Volatile fluxes during flood basalt eruptions and potential effects on the global environment: A Deccan perspective. *Earth Planet. Sci. Lett.* **248**, 518, 10.1016/j.epsl.2006.05.041 (2006).
29. N. Artemieva, J. Morgan, & Expedition 364 Science Party. Quantifying the release of climate-active gases by large meteorite impacts with a case study of Chicxulub. *Geoph. Res. Lett*., **44**, (10) 180–10, 188, doi.org/10.1002/2017GL074879 (2017).
30. B. J. Soden *et al*., Global Cooling After the Eruption of Mount Pinatubo: A Test of Climate Feedback by Water Vapor. Science, **296**, (5568) 727–730 (2002).
31. S. Kremser *et al.*, Stratospheric aerosol—Observations, processes, and impact on climate. *Reviews of Geophysics*, **54**, 278–335, https://doi.org/10.1002/2015RG000511 (2016).
32. M. B. Araújo *et al*., Standards for distribution models in biodiversity assessments. *Science Advances* **5**, eaat4858 (2019).
33. S. J. Phillips *et al*., Opening the black box: an open-source release of Maxent. *Ecography*. **40** (7), 887–893 (2017).
34. J. Elith *et al*., A statistical explanation of MaxEnt for ecologists. *Divers. Distrib*. **17**, 43–57 (2011).
35. M. W. Broadley *et al*., End-Permian extinction amplified by plume-induced release of recycled lithospheric volatiles. *Nature Geoscience*, **11**, 682–687 (2018). doi: 10.1038/s41561-018-0215-4
36. S. M. Holland. The stratigraphy of mass extinction and recoveries. *Annu. Rev. Earth Planet. Sci.* **48**:3.1-3.23, https://doi.org/10.1146/annurev-earth-071719-054827 (2020).
37. P. Shulte *et al.*, Response—Cretaceous Extinctions. *Science*, **328**, (5981) 975–976 10.1126/science.328.5981.975.
38. P. B. Wignall, Large igneous provinces and mass extinctions, *Earth Science Reviews*, **53**, 1–33, 10.1016/S0012-8252(00)00037-4 (2001).
39. R. V. White, A.D. Saunders. Volcanism, impact and mass extinctions: incredible or credible coincidences? *Lithos*, **79**, 299–316 (2005).
40. V. V. Kapur *et al*., Paleoenvironmental and paleobiogeographical implications of the microfossil assemblage from the Late Cretaceous intertrappean beds of the Manawar area, District Dhar, Madhya Pradesh, Central India. *Historical Biology*, **31**:9, 1145-1160 (2018).
41. V. R. Guntupalli and A. S. Prasad, Vertebrate fauna from the Deccan volcanic province: Response to volcanic activity. In Volcanism, Impacts, and Mass Extinctions: Causes and Effects, Gerta Keller, Andrew C. Kerr (2014).
42. N. R. Longrich *et al*., Severe extinction and rapid recovery of mammals across the Cretaceous–Palaeogene boundary, and the effects of rarity on patterns of extinction and recovery. *J. Evol. Biol*., **29**: 1495-1512, 10.1111/jeb.12882 (2016).

43. T. R. Lyson *et al*., Exceptional continental record of biotic recovery after the Cretaceous–Paleogene mass extinction, *Science*, 977-983 (2019).
44. G.P. Wilson. Mammalian faunal dynamics during the last 1.8 million years of the Cretaceous in Garfield County, *Montana. J. Mamm. Evol.* **12**: 53–76 (2005).
45. G.P. Wilson. Mammalian extinction, survival, and recovery dynamics across the Cretaceous-Paleogene boundary in northeastern Montana, USA. *Geol. Soc. Am. Spec. Pap*. **503**: 365–392 (2014).
46. C. M. Lowery *et al.*, Rapid recovery of life at ground zero of the End-Cretaceous mass extinction, *Nature*, 558, 288–291 (2018). 10.1038/s41586-018-0163-6.
47. B. Schaefer *et al*., Microbial life in the nascent Chicxulub crater. *Geology,* https://doi.org/10.1130/G46799.1 (2020).
48. S. L. Brusatte *et al.,* The extinction of the dinosaurs. *Biol. Rev.* **90**, 628–642 (2015).
49. J. D. Witts *et al*., Macrofossil evidence for a rapid and severe Cretaceous–Paleogene mass extinction in Antarctica, *Nat. Commun.* 10.1038/NCOMMS11738 (2016).
50. M. J. Henehan *et al.,* Rapid ocean acidification and protracted Earth system recovery followed the end-Cretaceous Chicxulub impact. *PNAS*, **116** (45) 22500-22504, 10.1073/pnas.1905989116 (2019).
51. J. Vellekoopet *al.,* Type-Maastrichtian gastropod faunas show rapid ecosystem recovery following the Cretaceous–Palaeogene boundary catastrophe. *Palaeontology*. doi:10.1111/pala.12462 (2019).
52. D.J. Field *et al.,* Early evolution of modern birds structured by global forest collapse at the end-Cretaceous mass extinction. *Current Biology*, **28**: 1-7, https://doi.org/10.1016/j.cub.2018.04.062 (2018).
53. N. R. Longrich *et al.,* Mass extinction of birds at the Cretaceous-Paleogene (K-Pg) boundary. *PNAS*, **108**(37):15253-7 (2011).
54. T. Halliday *et al.,* Eutherians experienced elevated evolutionary rates in the immediate aftermath of the Cretaceous–Palaeogene mass extinction. *Proc. R. Soc. B.*, **283**, 20153026, 10.1098/rspb.2015.3026 (2016)
55. T. J. Cleary *et al.,* Lepidosaurian diversity in the Mesozoic–Palaeogene: the potential roles of sampling biases and environmental drivers. *Proc. R. Soc. Lond. B.* (2018). doi: 10.1098/rsos.171830
56. N. R. Longrich *et al.,* Mass extinction of lizards and snakes at the Cretaceous-Paleogene boundary. *PNAS*. **109**, (52):21396-401 (2012).
57. P. M. Sheehan, D. E. Fastovsky. Major extinctions of land-dwelling vertebrates at the Cretaceous-Tertiary boundary, Eastern Montana. *Geology* **20**:556-60 (1992).
58. J. D. Archibald, J. J. Bryant. Differential Cretaceous–Tertiary extinction of nonmarine vertebrates; evidence from northeastern Montana. In: Sharpton VL, Ward PD, editors. Global catastrophes in earth history: An interdisciplinary conference on impacts, volcanism, and mass mortality. *GSA Special Paper*, 247:549-62 (1990).
59. M. J. Benton. Mass extinctions among tetrapods and the quality of the fossil record. *Proc. R. Soc. Lond. B.* 325:369–386 (1990).
60. L. J. Bryant. Non-dinosaurian lower vertebrates across the Cretaceous-Tertiary boundary in northeastern Montana. University of California Publications in Geological Sciences. **134**:1-107 (1989)
61. J. Sepkoski. A Compendium of Fossil Marine Animal Genera, *Bull. of Am. Paleontol.*, vol. **363**, edited by D. Jablonski , M. Foote, Paleontol. Res. Inst., Ithaca, N. Y (2002).
62. R. B. J. Benson, R. J. Butler. Uncovering the diversification history of marine tetrapods: ecology influences the effect of geological sampling biases. *Geol. Soc. Lond. Spec. Publ.* **358**: 191-208 (2011).
63. F. J. Mazzotti *et al.,* Large reptiles and cold temperatures: do extreme cold spells set distributional limits for tropical reptiles in Florida? *Ecosphere*, **7**(8), e01439, 10.1002/ecs2.1439 (2016).
64. G. C. Grigg *et al.*, Thermal relations of very large crocodiles, *Crocodylus porosus*, free-ranging in a naturalistic situation. *Proc. R. Soc. Lond. B.* **265**, 1793 -1799 (1998).

65. S. C. Andrew *et al.*, Clinal variation in avian body size is better explained by summer maximum temperatures during development than by cold winter temperatures. *The Auk: Ornithological Advances* 10.1642/AUK-17-129.1 (2018).
66. N. B. Grimm *et al.* The impacts of climate change on ecosystem structure and function. Frontiers in Ecology and the Environment, **11**, 474-482 doi:10.1890/120282 (2013).
67. F. C. Garcia *et al.* Changes in temperature alter the relationship between biodiversity and ecosystem functioning. *PNAS* **115** (43), 10989-10994, 10.1073/pnas.1805518115 (2018).
68. M. O'Leary *et al.* The placental mammal ancestor and the Post-K–Pg radiation of placentals. *Science*, **339**, 662–667 (2013).
69. N. R. Longrich *et al.* Biogeography of worm lizards (Amphisbaenia) driven by end-Cretaceous mass extinction. *Proc. R. Soc. Lond. B.* **202**, 20143034 (2015).
70. M. Joshi *et al.* Global warming and ocean stratification: A potential result of large extraterrestrial impacts, *Geophys. Res. Lett.* **44**, 3841– 3848, 10.1002/2017GL073330 (2017).
71. P. J. Valdes *et al.*, The BRIDGE HadCM3 family of climate models: HadCM3@Bristol v1.0. *Geosci. Model. Dev.* **10**, 3715-3743 (2017).
72. M. Collins, S. F. B. Tett, C. Cooper, The internal climate variability of HadCM3, a version of the Hadley Centre coupled model without flux adjustments. *Clim. Dynam.* **17**, 61-81 (2001).
73. D. J. Lunt *et al.*, Palaeogeographic controls on climate and proxy interpretation. Clim. Past. **12**, 1181-1198 (2016).
74. A. Marzocchi *et al.*, Orbital control on late Miocene climate and the North African monsoon: insight from an ensemble of sub-precessional simulations. *Clim. Past.* **11**, 1271-1295 (2015).
75. A. T. Kennedy, A. Farnsworth, D. J. Lunt, C. H. Lear, P. J. Markwick, Atmospheric and oceanic impacts of Antarctic glaciation across the Eocene-Oligocene transition. *Philos. T. R. Soc. A* 373 (2015).
76. D. J. Beerling, A. Fox, D. S. Stevenson, P. J. Valdes, Enhanced chemistry-climate feedbacks in past greenhouse worlds. *PNAS* **108**, 9770-9775 (2011).
77. C. G. Bardeen, R. R. Garcia, O. B. Toon, A. J. Conley, On transient climate change at the Cretaceous-Paleogene boundary due to atmospheric soot injections. PNAS **114**, E7415-E7424 (2017).
78. C. Covey, S. L. Thompson, P. R. Weissman, M. C. Maccracken, Global Climatic Effects of Atmospheric Dust from an Asteroid or Comet Impact on Earth. Global and Planetary Change **9**, 263-273 (1994).
79. D. L. Royer, M. Pagani, D. J. Beerling, Geobiological constraints on Earth system sensitivity to CO_2 during the Cretaceous and Cenozoic. *Geobiology* **10**, 298-310 (2012).
80. G. L. Foster, D. L. Royer, D. J. Lunt, Future climate forcing potentially without precedent in the last 420 million years. *Nat. Commun.* **8**, (2017).
81. S. Bekki *et al*., The role of microphysical and chemical processes in prolonging the climate forcing of the Toba eruption. *Geophys. Res. Lett.* **23**, 2669-2672 (1996).
82. D. J. Beerling *et al.,* An atmospheric pCO_2 reconstruction across the Cretaceous-Tertiary boundary from leaf megafossils. *PNAS*, **99** (12) 7836-7840 (2002).
83. J. D. O'Keefe, T. J. Ahrens. Impact production of CO_2 by the Cretaceous/Tertiary extinction bolide and the resultant heating of the Earth. *Nature*, 338, 247–249 (1989).
84. K. J. Hsü *et al.*, Mass mortality and its environmental and evolutionary consequences. Science, **216**, 249-256 (1982).
85. D. A. Kring and D. D. Durda, Trajectories and distribution of material ejected from the Chicxulub impact crater: Implications for postimpact wildfires. *J. Geophys. Res*. **107**, E8 (2002).
86. M. Joshi *et al.*, Global warming and ocean stratification: A potential result of large extraterrestrial impacts. *Geophys. Res. Lett.*, **44**, 3841– 3848 (2017).

87. M. Mussard et al, Modeling the carbon-sulfate interplays in climate changes related to the emplacement of continental flood basalts. *Geol. Soc. Am. Spec. Pap*. **505**, 339–352. (2014).
88. M. T. Jones, R. S. J. Sparks, P. J. Valdes, The climatic impact of supervolcanic ash blankets. *Clim. Dynam.* **29**, 553-564 (2007).
89. A. Guisan, U. Hofer, Predicting reptile distributions at the mesoscale: relation to climate and topography. *J. of Biogeog*. **30**, 1233–1243 (2003).
90. A. T. Peterson, Predicting species' geographic distributions based on ecological niche modeling. *Condor* **103**, 599–605 (2001).
91. A. T. Peterson, L. F. Ball, K. P. Cohoon. Predicting distributions of Mexican birds using ecological niche modelling methods. *Ibis* **144**, E27–E32 (2002).
92. W. Thuiller, D. Georges, R. Engler, biomod2: Ensemble platform for species distribution modeling. R package version 3.1-64 (2014). https://CRAN.R-project.org/package=biomod2
93. W. Thuiller, B. Lafourcade, R. Engler, M. B. Araujo, BIOMOD – A platform for ensemble forecasting of species distributions. *Ecography*, **32**, 369-373 (2009).

Figures and Tables

Figure 1. Geologic (a) and paleontological (b) records of the K/Pg mass extinction. Paleothermometer (a) showing the Deccan induced warming with the two main episodes of volcanism highlighted by the black arrows and symbols of volcanoes. The last phase endures the end of the Cretaceous, characterized by the bolide impact in Chicxulub. Fossil remains of non-avian dinosaurs (both body fossils, egg fragments and nesting sites) occur throughout the whole stratigraphic record of prolonged volcanism episodes (dinosaur silhouettes). Numbers in a represent Upper Maastrichtian dinosaur bearing localities, mapped on a Late Maastrichtian palaeogeography in B. 1, Hell Creek formation (USA); 2, Lameta formation (India); 3, Tremp Formation; 4, Couche III formation (Morocco); 5, Marilía formation (Brazil); 6, Nemegt formation (Mongolia).

738
739 **Figure 2.** K/Pg Surface temperature (°C) outputs from General Circulation Models (GCMs). Heat
740 maps represent temperature fluctuations from the late Maastrichtian control, with cooler
741 temperatures in blue and warmer in red. Late Maastrichtian climate control (a) is perturbed in (b)
742 by a solar dimming simulation reproducing the effect of mild asteroid impact or extreme
743 volcanism-induced cooling (b) at 5% (Sc 1) and of a more extreme asteroid-induced cooling
744 scenario (c) at 10% (Sc 2) of solar radiation reduction. The effect of prolonged volcanism is
745 reproduced with an increase to 1120 ppm of (d) CO_2 content (Sc 5) and to (e) 1680 ppm of CO_2
746 (Sc 6). A transient model including both Deccan volcanism and the effect of the Chicxulub impact
747 is shown in F (Sc 11) and G (Sc 12), and with inactive volcanism (H, Sc 13 and I, Sc 14), while
748 the 3 coldest years of the impact are modelled in F (Sc 11) and H (Sc 13; additional details and
749 figures on GCMs are in Supplementary material). Temperature scale running from -40 to 40 °C.
750
751

752
753 **Figure 3.** Ensemble habitat suitability models (averaged) projected globally for 9 clades of non-
754 avian dinosaurs (additional details and figures on habitat suitability models are in Supplementary
755 material). Blue color represents low level of habitat suitability (0), while red color represents high
756 habitability (1000). Habitat suitability models trained on the Late Maastrichtian record and GCMs
757 control (a), are then projected to decoupled solar dimming scenarios with 5% (Sc 1) of solar
758 reduction (b) and (Sc 2) 10% of solar reduction (c). A climatic scenario modelling two different
759 levels of greenhouse-enrichment due to the Deccan volcanism is reported in d (Sc 5) and e (Sc
760 6). The effect on the dinosaur suitable habitats for two transien simulations with Deccan
761 volcanism inactive (F, Sc 11 and G, Sc 12) and active (H, Sc 13 and I, Sc 14), shows the dynamic
762 response of global dinosaur habitability during the impact (F, Sc 11 and H, Sc 13) and throughout
763 the recovery (G, Sc 12 and I, Sc14).
764

765
766 **Figure 4.** Histogram showing areal amount of habitat suitability for different ensemble HSM
767 averaged in each climatic forcing scenarios (Sc) for all the clades used. A constant decrease from
768 initial conditions (Control) is observed in the solar dimming models (Sc 1, 5% and Sc 2, 10%). A
769 habitability increase is caused by a $\times 4CO_2$ (Sc 5) and $\times 6CO_2$ (Sc 6) addition. A transient model
770 shows the habitability decrease during the impact-related climatic perturbation and consequent
771 recovery, without Deccan volcanism (Sc 11 and Sc 12), and with active volcanism (Sc 13 and Sc
772 14).

773

774 **Table 1.** List of the K/Pg climate forcing scenarios used in this study. For the complete list check
775 Table S1. For a full description of all forcings please refer to Supplementary material.

Name in legends and text	Short description name	Description of simulation
Control	Maa_Cntrl	Late Maastrichtian Climate. Solar luminosity: 1357.18 W/m^2.
		Decoupled experiments
Scenario 1	Maa_-5%	5% solar dimming (modelling extreme Deccan cooling scenario or very mild Asteroid Impact scenarios). Solar luminosity: 1298.32 W/m^2
Scenario 2	Maa_-10%	10% solar dimming (Modelling lower extreme of impact-caused cooling). Solar luminosity: 1221.46 W/m^2.
Scenario 3	Maa_-15%	15% (Modelling moderate extreme of impact-caused cooling). Solar luminosity: 1153.6 W/m^2.
Scenario 4	Maa_-20%	20% (Modelling extreme of impact-caused cooling). Solar luminosity: 1085.74 W/m^2.
Scenario 5	Maa_4xCO_2	×4CO_2 (modelling 1120 ppm CO_2 injections caused by Deccan volcanism)
Scenario 6	Maa_6xCO_2	×6CO_2 (modelling 1680 ppm CO_2 injections caused by Deccan volcanism)
		Coupled experiments (transient)
Scenario 11	Aero100x_+Ash	Aerosol+Ash, During-Impact, ×100 Pinatubo
Scenario 12	Post_Aero100x_+Ash	Aerosol+Ash, Post-Impact, ×100 Pinatubo
Scenario 13	Aero100x_+4CO_2_+Ash	Aerosol+Ash+Deccan, During-Impact ×100 Pinatubo
Scenario 14	Post_Aero100x_+4CO_2_+Ash	Aerosol+Ash+Deccan, Post-Impact ×100 Pinatubo

776
777
778

Table 2. K/Pg climate forcing scenarios. The end-Cretaceous climate of the Maastrichtian (control) and perturbations to the mean climate state resulting from a set of solar luminosity (W/m2) reduction experiments at -5% and -10% (additional experiments are presented in Supplementary material) and two different scenarios of CO2 injection due to Deccan volcanism. Data are shown for Sea Surface Temperatures (SST; °C) at intermediate (666 m) ocean water column depth; global, land and ocean Surface Air Temperatures (SAT; °C); and global, land and ocean precipitation (mm/day) for the mean of the last 50-years of each simulation (see expanded methods in Supplementary material).

	Ocean temperature		SAT			Precipitation		
Experiment	SST	666m depth	Ocean	Land	Global	Ocean	Land	Global
Control	22.64	12.41	21.65	11.49	18.96	3.5	2.38	3.2
-5% Sol. (Sc1)	16.93	12.06	14.87	1.83	11.42	3	2.05	2.75
-10% Sol. (Sc2)	11.06	11.72	4.56	-12.18	0.13	2.5	1.59	2.26
$2xCO_2$>$4xCO_2$ (Sc5)	25.11	12.56	24.47	16.2	22.28	3.58	2.49	3.29
$2xCO_2$>$6xCO_2$ (Sc6)	27.02	12.66	26.86	20.24	25.11	3.59	2.5	3.3

Table 3. Transient aerosol K/Pg extinction simulations. A set of transient simulations with perturbed aerosol atmospheric optical depth, pCO_2 concentrations and ash layer deposits is performed over a set of 200-year simulations. Their individual global, land and oceanic impact on specific climate variables (SST [°C], SAT [°C], Precipitation [mm/day]) for the 50-year mean pre-impact climate state and the mean of the 3 coolest years resulting from the post-asteroid impact. The complete set of experiments with sensitivity tests is presented in Supplementary material.

	SST		666 m depth:		SAT						Precipitation					
					Ocean		Land		Global		Ocean		Land		Global	
Experiment	Before Impact	Impact	Before Impact	Impact	Before Impact	Impact	Before Impact	Impact	Before Impact	Impact	Before Impact	Impact	Before Impact	Impact	Before Impact	Impact
Aerosol 100 with Ash deposit (Sc11-12)	22.1	2.49	11.81	11.88	21.38	-13.44	10.99	-30.21	18.63	-17.87	3.52	0.78	2.4	0.28	3.22	0.65
Aerosol 100 and 2xCO_2 >4xCO_2 with Ash deposit (Sc13-14)	23.93	4.05	11.81	11.88	23.59	-8.23	14.95	-25.96	21.31	-12.92	3.59	0.91	2.51	0.33	3.31	0.75